NAVAL POSTGRADUATE SCHOOL

MONTEREY, CALIFORNIA

THESIS

SOURCE LOCALIZATION IN A COGNITIVE RADIO ENVIRONMENT CONSISTING OF FREQUENCY AND SPATIAL MOBILITY

by

Agur Adams

December 2011

Thesis Co-Advisors:	Murali Tummala
	John McEachen
Second Reader:	Frank Kragh

Approved for public release; distribution is unlimited.

THIS PAGE INTENTIONALLY LEFT BLANK

REPORT DOCUMENTATION PAGE			*Form Approved OMB No. 0704-0188*
Public reporting burden for this collection of information is estimated to average 1 hour per response, including the time for reviewing instruction, searching existing data sources, gathering and maintaining the data needed, and completing and reviewing the collection of information. Send comments regarding this burden estimate or any other aspect of this collection of information, including suggestions for reducing this burden, to Washington headquarters Services, Directorate for Information Operations and Reports, 1215 Jefferson Davis Highway, Suite 1204, Arlington, VA 22202-4302, and to the Office of Management and Budget, Paperwork Reduction Project (0704-0188) Washington DC 20503.			
1. AGENCY USE ONLY *(Leave blank)*	**2. REPORT DATE** December 2011	**3. REPORT TYPE AND DATES COVERED** Master's Thesis	
4. TITLE AND SUBTITLE Source Localization in a Cognitive Radio Environment Consisting of Frequency and Spatial Mobility			**5. FUNDING NUMBERS**
6. AUTHOR(S) Agur Adams			
7. PERFORMING ORGANIZATION NAME(S) AND ADDRESS(ES) Naval Postgraduate School Monterey, CA 93943-5000			**8. PERFORMING ORGANIZATION REPORT NUMBER**
9. SPONSORING /MONITORING AGENCY NAME(S) AND ADDRESS(ES) N/A			**10. SPONSORING/MONITORING AGENCY REPORT NUMBER**
11. SUPPLEMENTARY NOTES The views expressed in this thesis are those of the author and do not reflect the official policy or position of the Department of Defense or the U.S. Government. IRB Protocol Number N/A			
12a. DISTRIBUTION / AVAILABILITY STATEMENT Approved for public release; distribution is unlimited.			**12b. DISTRIBUTION CODE** A

13. ABSTRACT (maximum 200 words)

Cognitive radio presents a unique challenge to source localization in that the radio has the ability to adapt to the environment, thus rendering current localization techniques ineffective due to a shifting combination of spatial, frequency, and temporal parameters. For any localization scheme to be effective, it must be able to adapt over time as a cognitive radio adapts to its surroundings. In this thesis an extended semi range-based localization scheme is proposed to accomplish this task. The proposed scheme estimates the position of a cognitive radio using the collaborative spectrum sensing results of a wireless radio frequency sensor network in a cognitive radio environment. The central idea behind the proposed scheme is to exploit the relationships between spatial, frequency, and temporal parameters of the environment to solve for the position of the cognitive radio. The proposed scheme is modeled in the MATLAB programming language, and its efficacy is demonstrated through simulation. It is shown that over time the proposed scheme is capable of estimating the frequency band of operation and the location of a cognitive radio, and is thus capable of accounting for both frequency and spatial mobility inherent in the cognitive radio environment.

14. SUBJECT TERMS Cognitive Radio, Source Localization, Semi Range-Based Localization, Mobile Positioning, Wireless Sensor Networking			**15. NUMBER OF PAGES** 104
			16. PRICE CODE
17. SECURITY CLASSIFICATION OF REPORT Unclassified	**18. SECURITY CLASSIFICATION OF THIS PAGE** Unclassified	**19. SECURITY CLASSIFICATION OF ABSTRACT** Unclassified	**20. LIMITATION OF ABSTRACT** UU

NSN 7540-01-280-5500 Standard Form 298 (Rev. 2-89)
Prescribed by ANSI Std. 239-18

THIS PAGE INTENTIONALLY LEFT BLANK

Approved for public release; distribution is unlimited

SOURCE LOCALIZATION IN A COGNITIVE RADIO ENVIRONMENT CONSISTING OF FREQUENCY AND SPATIAL MOBILITY

Agur S. Adams
Captain, United States Marine Corps
B.S., United States Naval Academy, 2003

Submitted in partial fulfillment of the
requirements for the degree of

ELECTRICAL ENGINEER
and
MASTER OF SCIENCE IN ELECTRICAL ENGINEERING

from the

NAVAL POSTGRADUATE SCHOOL
December 2011

Author: Agur Adams

Approved by: Murali Tummala
Thesis Co-Advisor

John McEachen
Thesis Co-Advisor

Frank Kragh
Second Reader

Ralph Robertson
Chair, Department of Electrical and Computer Engineering

THIS PAGE INTENTIONALLY LEFT BLANK

ABSTRACT

Cognitive radio presents a unique challenge to source localization in that the radio has the ability to adapt to the environment, thus rendering current localization techniques ineffective due to a shifting combination of spatial, frequency, and temporal parameters. For any localization scheme to be effective, it must be able to adapt over time as a cognitive radio adapts to its surroundings. In this thesis an extended semi range-based localization scheme is proposed to accomplish this task. The proposed scheme estimates the position of a cognitive radio using the collaborative spectrum sensing results of a wireless radio frequency sensor network in a cognitive radio environment. The central idea behind the proposed scheme is to exploit the relationships between spatial, frequency, and temporal parameters of the environment to solve for the position of the cognitive radio. The proposed scheme is modeled in the MATLAB programming language, and its efficacy is demonstrated through simulation. It is shown that over time the proposed scheme is capable of estimating the frequency band of operation and the location of a cognitive radio, and is thus capable of accounting for both frequency and spatial mobility inherent in the cognitive radio environment.

THIS PAGE INTENTIONALLY LEFT BLANK

TABLE OF CONTENTS

LIST OF FIGURES

LIST OF TABLES

THIS PAGE INTENTIONALLY LEFT BLANK

LIST OF SYMBOLS AND ACRONYMS

α	path loss
a	horizontal Cartesian coordinate of a sensor node
A	number of observed energies within an energy detection region
b	vertical Cartesian coordinate of a sensor node
β	weighting coefficient for the probability of false alarm
c	coefficient representing all other factors influencing received signal power
ϑ_s	Gaussian random variable used to control the shadowing effect
d	distance
ε	tolerance level between iterations of non-linear least squares method
f	frequency
γ	instantaneous signal-to-noise ratio
i	sensor node number
j	spectral scan number
κ	scalar used to adjust the Gauss-Newton direction
k	channel number
K	total number of channels
λ	energy detection threshold
l	iteration number of non-linear least squares method
L	performance parameter to be optimized
n	number of bits
σ_0^2	noise variance
N	total number of sensor nodes
N_P	total number of spectral scans
p	received signal power
p_b	primary user 'busy' state transition probability
p_i	primary user 'idle' state transition probability
p_r	secondary user fast sense probability
p_v	secondary user fine sense probability
φ	angle of the sensor node
P_d	probability of detection
P_f	probability of false alarm
P_{tx}	transmission power of user
ς	cyclic frequency
s	instantaneous received signal
S	shadowing constant
t	time
T	time interval
u	time-bandwidth product

w	weighting value
W	bandwidth
x	received signal
ξ_{RMSE}	root-mean-square error
X	received signal energy

AOA	Angle of Arrival
BS	Base Station
CPE	Customer Premise Equipment
DoD	Department of Defense
DSA	Dynamic Spectrum Access
ESRB	Extended Semi Range-Based
FCH	Frame Control Header
FDMA	Frequency Division Multiple Access
GPS	Global Positioning System
IEEE	Institute of Electrical and Electronics Engineers
ISRB	Iterative Semi Range-Based
JTRS	Joint Tactical Radio System
MAC	Medium Access Control
NLSM	Non-linear Least Squares Method
NLOS	Non-Line-of-Sight
OFDMA	Orthogonal Frequency-Division Multiple Access
PHY	Physical
PDF	Probability Density Function
PSRB	Practical Semi Range-Based
QP	Quiet Periods
RF	Radio Frequency
RMSE	Root-Mean-Square Error
RSS	Received Signal Strength
SCH	Superframe Control Header
SNR	Signal-to-Noise Ratio
TDOA	Time Difference of Arrival
TOA	Time of Arrival
TV	Television
WG	Working Group
WRAN	Wireless Regional Area Network

EXECUTIVE SUMMARY

Presently, a growing conflict is emerging between the low utilization and increasing scarcity of electromagnetic spectrum around the globe. Cognitive radio is considered the primary solution to this problem as a cognitive radio is capable of opportunistically seizing underutilized portions of the electromagnetic spectrum (i.e., white spaces) by adapting the radio's attributes to match the available resources. With such communication advancements rapidly developing, it is critical for the Department of Defense (DoD) to remain aware of the positioning techniques being utilized within these networks. Furthermore, in the context of cyber warfare, it is crucial for the DoD to develop and enhance cognitive radio source localization techniques as cognitive radio can be adopted for military applications by adversaries and pose potential security risks if used internally. Given these concerns, an effective solution to cognitive radio source localization is needed.

The objective of this thesis is to estimate the position of a cognitive radio using the collaborative spectrum sensing results of a wireless radio frequency (RF) sensor network in a cognitive radio environment. In the context of cognitive radio, the environment consists of two types of users. First, a primary user has principle rights to the frequency spectrum but may not completely exhaust the resources available in the area. Therefore, a secondary user network may also exist which can opportunistically use the available frequency spectrum leftover from the primary user network by employing cognitive radio technology.

An extension of the semi range-based localization algorithm is proposed in this thesis to accomplish the aforementioned objective. Semi range-based localization, originally proposed for primary user source localization in cognitive radio networks, is extended to secondary user source localization in this thesis. The proposed extended semi range-based (ESRB) localization scheme utilizes *n*-bit spectrum sensing in the spectrum sensing process and semi range-based localization in the localization process.

The proposed scheme was modeled in the MATLAB programming language and its efficacy demonstrated through simulation. Power estimation and the effects of *n*-bit spectrum sensing, the number of spectral scans per superframe, the number of superframes, and the number and position of sensor nodes were examined to determine the effect on the secondary user position estimate. Frequency and spatial mobility of the secondary user were also examined to account for all possible variations in the secondary user's activity. Scalability of the ESRB localization scheme was also addressed with multiple secondary users present in the environment.

Simulation results demonstrated that over time the proposed scheme is capable of estimating the frequency band of operation and the location of a cognitive radio. The number of sensor nodes did not directly influence position estimation accuracy; however, adequate spatial separation among the sensor nodes proved to be a significant factor in the performance of the localization process. Similar to position estimation, power estimation also improved as the number of samples from the sensor network increased. As the number of superframes increased and more decision data became available, the proposed scheme was capable of refining the position estimate using relevant decision data to deliver accurate results.

Alternatively, the use of *n*-bit spectrum sensing significantly improved the performance of the ESRB localization scheme in terms of divergence percentage. The decrease in divergence percentage also directly influenced the overall position estimation error, which allowed the proposed scheme to perform well with a limited amount of decision data from the sensor network.

Finally, through instantaneous results, it was shown the ESRB localization is scalable to localize multiple secondary users in the environment and is capable of accounting for both frequency and spatial mobility when the secondary user is mobile. Limited frequency and spatial tracking was demonstrated for a mobile secondary user on a fixed trajectory at constant speed. Frequency and spatial estimation was accomplished through repeated application of the proposed ESRB localization scheme.

ACKNOWLEDGMENTS

I would like to offer my gratitude to Professor Murali Tummala, Professor John McEachen, and Professor Frank Kragh of the Naval Postgraduate School, Monterey, California for their invaluable instruction and contributions to this work.

I would also like to thank my wife, Krista, for her loving support, patience, commitment, and encouragement during the course of my master's work and in our marriage.

Finally, I would like to thank my local church and small group community for their prayers, thoughts, and support throughout my time at the Naval Postgraduate School.

THIS PAGE INTENTIONALLY LEFT BLANK

I. INTRODUCTION

Presently, a growing conflict is emerging between the low utilization and increasing scarcity of electromagnetic spectrum around the globe [1], [2]. The popularity of unlicensed bands has proven to be an effective solution to development and deployment of new wireless networks but has not abated the increasing demand for wireless spectrum [1]. Cognitive radio is considered the primary solution to this problem as a cognitive radio is capable of opportunistically seizing underutilized portions of the electromagnetic spectrum (i.e., white spaces) by adapting the radio's attributes to match the resources available [1–6]. This is accomplished through two primary means: 1) spectral sensing of the environment and 2) informed decision making [3], [6]. The combination of awareness and decision making is the foundation for cognition in the system and distinguishes a cognitive radio from any other type of communications technology [2], [7], [8].

Future Department of Defense (DoD) communication technologies will depend heavily on the principles inherent in cognitive radio (e.g., dynamic spectrum access (DSA) in the Joint Tactical Radio System (JTRS) [9]) due to the growing spectrum shortage and the need for DoD operations to be less invasive when working in a counter-insurgency or multi-national environment [9–12]. With such communication advancements rapidly developing, it is critical for the DoD to remain aware of the positioning techniques being utilized within these networks. Furthermore, in the context of cyber warfare, it is crucial for the DoD to develop and enhance cognitive radio source localization techniques as cognitive radio can be adopted for military applications by adversaries and pose potential security risks if used internally. Given these concerns, an effective solution to cognitive radio source localization is needed.

Wireless radio frequency (RF) sensor networks offer a promising solution to the aforementioned problem [13], [14]. Low-powered and cost effective, a wireless RF sensor network can be deployed in a hostile or non-hostile area to detect signals of interest through spectrum sensing and aid in localization of a specific target [13–16]. Such a scenario is shown in Figure 1, where multiple sensor nodes are deployed in an

environment to detect the presence of an emitter of interest. In the context of cognitive radio, the environment consists of two different types of users [3], [6]. As shown in Figure 1, the present primary user has principle rights to the frequency spectrum in that geographical area [3], [5]. The primary user network operates without knowledge or coordination with any other type of user in the environment but may not completely exhaust the resources available in the area [3], [5], [6], [17]. Therefore, a secondary user network also exists which can opportunistically use the available frequency spectrum leftover from the primary user network by employing cognitive radio technology [3], [5]. The secondary user has the responsibility to prevent interference with the primary user [3], [5]. A scenario where the secondary user is the target and a wireless RF sensor network is available to aid in localization is adopted in this thesis.

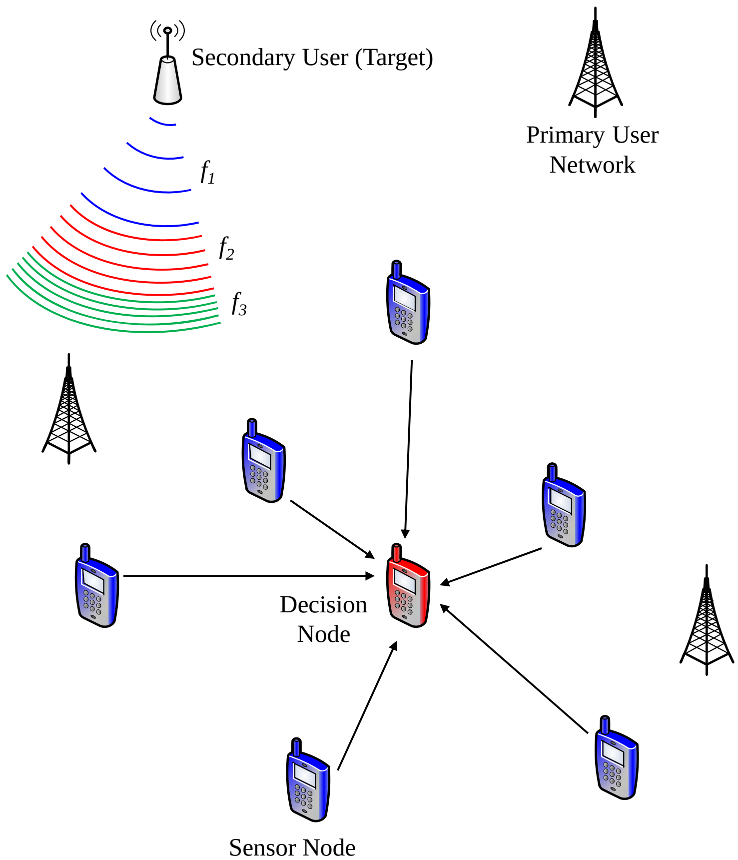

Figure 1. Overall scenario using a wireless RF sensor network to determine the frequency bands and location of a cognitive radio.

A. THESIS OBJECTIVE

The objective of this thesis is to estimate the position of a cognitive radio using the collaborative spectrum sensing results of a wireless RF sensor network in a cognitive radio environment. In order to accomplish this objective, several additional tasks must be achieved. First, any scheme used to localize the cognitive radio must be capable of tracking the frequency usage of the cognitive radio over time. Second, any localization scheme must be able to decipher between the secondary users and primary users of the frequency spectrum. Third, given additional spectrum sensing results from the wireless sensor network, the localization scheme must have some method of position refinement to converge to the true position of the cognitive radio.

An extension of the semi range-based localization algorithm [5], [17] is proposed in this thesis to accomplish these objectives. Semi range-based localization was originally proposed for primary user source localization in cognitive radio networks [5], [17] but is extended to secondary user source localization. The proposed extended semi range-based (ESRB) localization scheme utilizes *n*-bit spectrum sensing in the spectrum sensing process [18] and semi range-based localization [5], [17] in the localization process. The proposed scheme will be modeled in the MATLAB programming language and its efficacy demonstrated through simulation.

B. RELATED WORK

Multiple technologies, such as the Institute of Electrical and Electronics Engineers (IEEE) standard 802.22 [1], [19], [20] and IEEE standard 802.11af [20], are being built to take advantage of cognitive radio. Concurrently with their development, several techniques have been proposed for primary user source localization by a secondary user network [5], [6], [17]. However, very little work is being done in regards to cognitive radio source localization [21]. Current source localization techniques are rendered ineffective in the context of cognitive radio due to a shifting combination of spatial, frequency, and temporal parameters [5], [21]. One potential solution to this problem is semi range-based localization.

Originally proposed by Ma et al. in [5] for primary user source localization, semi range-based localization has an adaptive quality inherent in the localization process for use in cognitive radio networking. In [17], Wang et al. have extended the localization algorithm proposed in [5] to remove any requirement for cooperation among the secondary and primary user networks in the localization process. Both proposed semi rang-based localization algorithms make use of binary spectrum sensing to facilitate localization [5], [17].

Spectrum sensing and cooperation in spectrum sensing remains an active area of research [2], [18]. Recently, two-bit and three-bit hard combination were proposed for use in wireless RF sensor networks to improve the overall detection performance of a sensor network [18], [22]. The two-bit and three-bit hard combination schemes presented in [18] and [22] for *n*-bit spectrum sensing and the semi range-based localization algorithms presented in [5] and [17] for the ESRB localization scheme are used in this thesis.

C. THESIS OUTLINE

The outline of this thesis is as follows. Background on spectrum sensing and localization using a wireless RF sensor network along with an application area of these two concepts is provided in Chapter II. The ESRB localization is described in detail and the fundamental methods used in the proposed scheme are presented in Chapter III. The simulation scenario and simulation model used to implement the ESRB localization scheme along with simulation results are presented in Chapter IV. A summary of the work completed, a summary of significant results, and ideas for future work are presented in Chapter V. The MATLAB code used to support the work completed is given in the appendix.

II. BACKGROUND

A brief introduction to the problems encountered with source localization of a cognitive radio was provided in Chapter I. Two broad areas were identified as part of the solution to the problem: 1) spectrum sensing and 2) localization using a wireless RF sensor network. Background on each of these areas and an implementation of these techniques in a specific application are presented in this chapter.

A. SPECTRUM SENSING

In general, spectrum sensing is the process of gaining awareness of the frequency usage and presence of users within a geographical area [2]. Typically, this involves examining a portion of the frequency spectrum through a selected method over an interval of time to identify whether or not the frequency spectrum is in use [2], [8]. In the context of cognitive radio, such awareness can be obtained through local measurements performed by the cognitive radio or through external resources independent of the radio itself (e.g., using a table lookup in a geo-location frequency occupancy database) [2], [8].

1. Spectrum Sensing Methods

Several methods have been proposed to perform local spectrum sensing [2], [8], [18], [22]. The following section highlights three of the most relevant methods from the literature [22]: 1) energy detection based spectrum sensing, 2) cyclostationary-based spectrum sensing, and 3) matched filtering. A brief overview of each technique is provided below along with the relative advantages and disadvantages of each.

a. Energy Detection Based Spectrum Sensing

Due to its low complexity and computational cost, energy detection based spectrum sensing is the most common spectrum sensing method [2]. It is performed by comparing the received energy of the signal against a predefined energy detection threshold to determine the presence or absence of the user in the frequency band of interest [2], [8], [23]. The energy of the received signal is determined by squaring and integrating the received signal strength (RSS) over the observation time interval [2], [8],

[23]. The energy detection threshold is determined using the noise variance of the environment [8]. Thus, small errors in the noise variance estimation can cause significant performance degradation [8]. Energy detection based spectrum sensing is the optimal detection method for zero-mean constellation signals when no information is known in advance about the user occupying the channel [8], [23]. However, energy detection based spectrum sensing cannot distinguish the type of user occupying the frequency band [2], [8]. In addition, under low signal-to-noise ratio (SNR) conditions, energy detection performs poorly [2], [8].

b. Cyclostationary-Based Spectrum Sensing

Given the disadvantages of energy detection based spectrum sensing, cyclostationary-based spectrum sensing offers an attractive alternative [2], [8]. By exploiting the cyclostationary features of the received signal [2], cyclostationary-based spectrum sensing is capable of discriminating which type of user is present [2], [8] and detecting the presence of a user under low SNR conditions [8]. Such benefits come at the cost of additional hardware complexity and a lengthier detection process when compared to energy detection based spectrum sensing [8]. Cyclostationary features are the result of periodicity in the received signal or its statistical properties [2]. As such, detection is accomplished by finding the unique cyclic frequency of the spectral correlation function of the received signal [2], [8]. The spectral correlation function is determined by taking the Fourier transform of the cyclic autocorrelation function. The spectral correlation function is given by [2]

$$S(f,\varsigma) = \int_{-\infty}^{\infty} R_x^{\varsigma}(\tau) e^{-j2\pi f\tau} d\tau \tag{1}$$

where the cyclic autocorrelation function is determined by [8]

$$R_x^{\varsigma}(\tau) = E\left\{x(t+\tau)x^*(t-\tau)e^{-j2\pi\varsigma t}\right\} \tag{2}$$

where $x(t)$ is the received signal and ς is the cyclic frequency [8]. Under cyclostationary-based spectrum sensing, *a priori* knowledge of the cyclostationary features of the received signal is required for successful detection [2], [8]. However, if

complete knowledge of the received signal is known in advance, matched filtering based spectrum sensing provides the optimal solution [2], [8].

c. Matched Filtering

Matched filtering is the optimal solution when complete *a priori* knowledge of the received signal is available [2], [8]. It is achieved by correlating the received signal with the known signal to be detected [2], [8]. In this way, the SNR of the received signal is maximized [8]. An additional benefit is the short time period necessary to achieve a specific probability of false alarm or probability of missed detection relative to energy detection or cyclostationary-based spectrum sensing [2]. However, the requirement for complete *a priori* knowledge of the signal is a significant drawback to this method given this information may not always be available in advance [2], [8]. Further, to detect a large number of different signals, a separate matched filter must be used for each different signal [2], [8]. Thus, hardware complexity is a significant factor in implementation when detecting a large number of different signals [2].

2. Cooperative Spectrum Sensing

Local spectrum sensing methods using distributed sensor nodes are limited in their effectiveness due to irregularities in the environment [2], [8], [22]. Multipath fading and non-line-of-sight (NLOS) conditions can significantly reduce the probability of detecting whether or not a user is present in the frequency band of interest at a single sensor node [8], [22]. Most damaging to the spectrum sensing process is the problem of the hidden node [8], which occurs when a particular sensor node suffers from NLOS conditions or severe multipath fading as shown in Figure 2. The two sensor nodes experiencing multipath fading and NLOS conditions may not detect the presence of the user. However, if the sensor nodes were to share their information with each other through a central decision node as illustrated in the figure, a more accurate global result may be achieved [8]. Such collaboration among the sensor nodes to overcome local environmental effects is the essence of cooperative spectrum sensing [8].

Cooperative spectrum sensing can be summarized in three primary steps [23]. First, each sensor node performs local spectrum sensing at its position and determines

whether or not the frequency band of interest is occupied [23]. Second, all sensor nodes transmit their spectrum sensing decisions to a central decision maker [23]. Third, the decision maker aggregates the individual local spectrum sensing decisions and makes a final global decision as to the presence or absence of a user based on a decision rule [23].

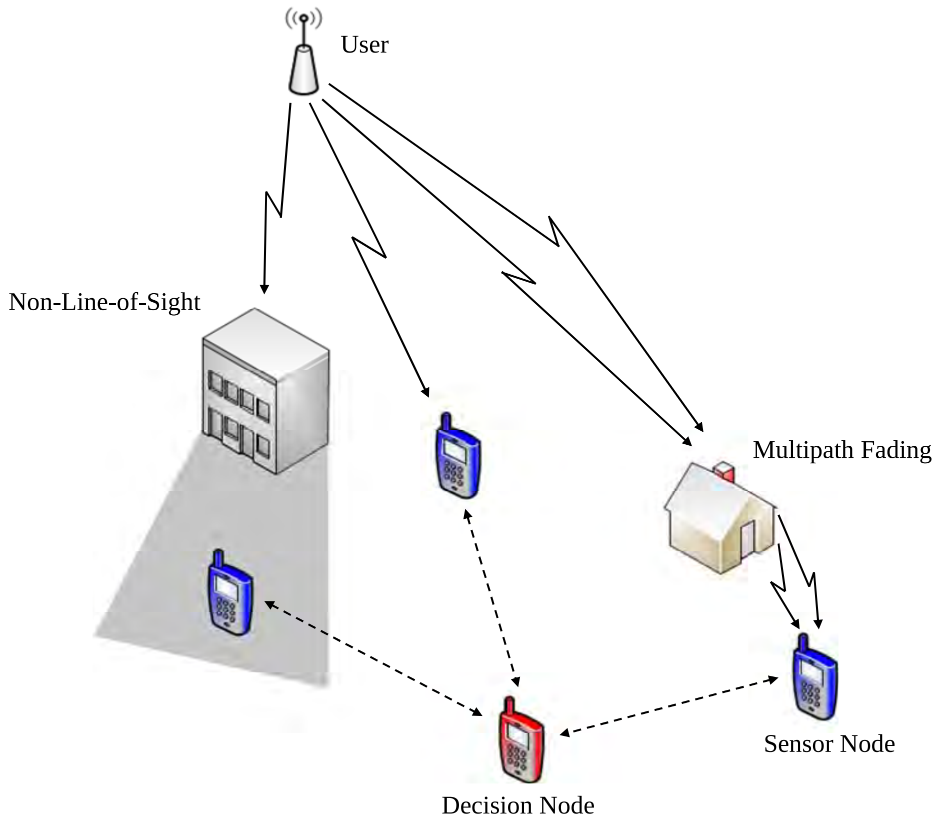

Figure 2. Illustration of cooperative spectrum sensing under shadowing and multipath fading.

The benefit of cooperation in the spectrum sensing process necessitates employing a wireless RF sensor network to estimate the position of a cognitive radio. Cooperative spectrum sensing has proven to be an effective solution to overcome the aforementioned environmental effects [5], [8], [17], [22], [24]. This is achieved through spatial separation in the collective decisions of the received signal of interest from all sensor nodes [8]. The detection performance gain from spatial separation makes detection possible where it was once unachievable through local spectrum sensing alone [8]. In addition to overcoming environmental effects, cooperative spectrum sensing

increases the detection sensitivity of the overall network without the requirement for each sensor node to have high detection sensitivity [18], [24].

The benefits gained by cooperative spectrum sensing are costly [18], [24]. For collaboration to occur among the sensor nodes, some form of communication must happen, resulting in overhead to the spectrum sensing process [8], [24]. Additionally, some form of a control channel must be established to facilitate communication among the sensor nodes [8], [24]. The control channel may also be subject to the same adverse environmental conditions [8], [24]. Two classes of techniques have been proposed to address communication in cooperative spectrum sensing [8], [18], [22].

a. Hard and Soft Combination

Hard combination and soft combination are the two primary techniques by which cooperative spectrum sensing is conducted [8], [22]. In hard combination, also referred to as decision fusion [8], the local spectrum sensing decisions of each sensor node are transmitted to a decision node where they are fused into a global decision [8], [22]. Each sensor node must make a local decision declaring the presence or absence of the user [8], [17]. The local decision then results in a single bit being transmitted by each sensor node indicating its decision [8], [22]. Next, the global decision can be determined by a number of different fusion rules [23]. For example, the decision node may use a logical OR rule where if one sensor node declares the user present, the global decision is the user is present [8], [23]. By only transmitting the local decision from each sensor node, hard combination offers very little communication overhead [8], [22]. However, improved detection performance can be achieved when additional information is available [8], [22].

In soft combination, also referred to as data fusion, the original sensing measurement data is transmitted to the decision maker without a local decision being made by the sensor nodes [8], [22]. Rather, the decision node is the only entity responsible for making a decision [8], [22]. In the context of energy based spectrum sensing, the measurement data from each sensor node is weighted and summed in accordance with the instantaneous SNR at that sensor node to determine the overall

energy in the frequency band of interest [22]. It has been shown that soft combination outperforms hard combination in terms of detection performance using energy based spectrum sensing [22]. Such gains come at the expense of additional communication overhead [22]. To strike a balance in the performance-communication tradeoff between hard and soft combination, hybrid solutions have been proposed to take advantage of the benefits of both schemes [22].

b. Two-bit Hard Combination Scheme

Two-bit hard combination is considered a softened hard combination scheme where two bits are used to represent the local spectrum sensing decision of each sensor node [22]. As with soft combination, two-bit hard combination is applied in the context of energy detection based spectrum sensing [22]. Three energy detection thresholds are defined to break up the range of observed energy into four regions as shown in Figure 3 [22]. Each region is assigned a specific weight w_i in accordance with L, a performance parameter to be optimized. Given the four energy regions defined, each sensor node must use two bits to represent the region of energy detected [22]. The energy detection thresholds are represented by $\lambda_1, \lambda_2,$ and λ_3 in Figure 3 [22].

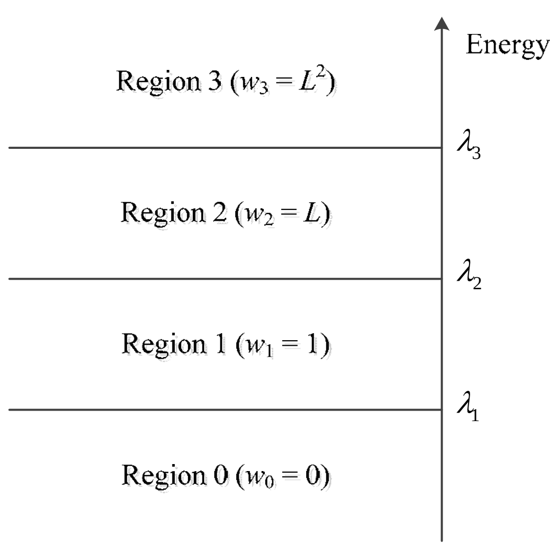

Figure 3. Energy regions of the two-bit hard combination scheme (From [22]).

Similar to soft combination, two-bit hard combination uses a weighted summation to develop the global decision [22]. The decision as to whether the user is present or absent in the frequency band of interest, is given by [18]

$$\sum_{i=0}^{3} w_i A_i \geq L^2 \tag{3}$$

where A_i is the number of observed energies falling in region *i* over the sensing period [22]. The detection performance of two-bit hard combination is comparable with that of soft combination using equal gain combining [22]. Such an improvement in performance with little cost in communication overhead has motivated consideration of additional bits in the two-bit hard combination scheme [18]. In [18], three-bit hard combination is proposed for cooperative wideband spectrum sensing using RF sensor networks. It is shown that three-bit hard combination outperforms traditional hard combination in false alarm performance [18].

B. LOCALIZATION USING WIRELESS RADIO FREQUENCY SENSOR NETWORKS

To date, numerous propagation model-based localization schemes have been proposed to enable a wireless device to find its own position or the position of other devices [3], [6]. Such schemes can be broken down into two main categories: 1) range-based and 2) range-free [5], [6]. The means by which position estimation is achieved distinguishes these two categories from one another [3], [5], [6].

1. Range-Based Localization Schemes

Position estimation occurs in two phases under range-based localization schemes: 1) ranging and 2) localization [25]. In the ranging phase, point-to-point ranging estimations are made between a transmitter and receiver using metrics such as time-of-arrival (TOA), time-difference-of-arrival (TDOA), angle-of-arrival (AOA), RSS, and others [3], [5], [6]. During the localization phase, the distances obtained in the ranging phase are translated into position through the intersection of three or more estimated distances from known positions [25].

TOA is obtained from the internal clock of the receiver when the signal of interest arrives at its terminals [3]. Therefore, the degree of precision in the receiver's clock is one of the greatest factors which can create error in TOA observations [3]. To convert TOA into distance, the receiver and transmitter's clock must be perfectly synchronized [3], [25]. The estimated TOA at the receiver is the sum of the transmission time, the propagation delay, and the error in the transmitter and receiver's clock synchronization [3]. Distance is obtained from the propagation delay between the transmitter and receiver [3], [25].

To alleviate the requirement for clock synchronization between the transmitter and receiver, TDOA-based methods utilize the difference between multiple TOA measurements [25]. This may be the difference in TOA for a single signal to reach multiple receivers, or the difference in TOA for multiple signals from one transmitter to reach one receiver [25]. Thus, TDOA-based methods require synchronization between receivers but not between transmitter and receiver [3], [25].

AOA-based schemes utilize the angle at which the transmitter's signal arrives at the receiver to estimate distance [3], [25]. To this end, directional antennas are required which can significantly increase cost and complexity [3], [25]. AOA-based methods are also strongly susceptible to adverse environmental effects such as multipath fading and shadowing [3], [25].

As a low cost solution, RSS-based methods offer an effective alternative to the disadvantages of AOA-based methods [25]. Its low cost is attributed to the fact that most receivers are capable of performing RSS measurements [25], and it is simple to implement in hardware [26]. Given an accurate propagation model, the RSS can be used to estimate the distance between the transmitter and the receiver [3], [25]. The RSS is a measurement of the magnitude of the signal power observed by the receiver [3], [26]. This measurement is also subject to significant deviations due the aforementioned environmental effects [3], [25].

2. Range-Free Localization Schemes

In the context of wireless sensor networking, range-free schemes are used to determine the position of the sensor nodes within the network [3], [5], [6], [16]. Multiple anchor nodes with known positions are used as the basis to determine the position of other sensor nodes [16], [27]. This is accomplished through such metrics as hop count or proximity vice triangulation or trilateration as in range-based localization schemes [27]. As a result, less hardware is required for individual devices to be positioned [16]. However, this also degrades the overall accuracy in the position estimate [3], [6]. Range-based schemes require more hardware in the sensor node in order to deliver precise measurements for position estimation [16], [27].

Ultimately, both classes of schemes fall short in cognitive radio source localization because they lack the ability to adapt as the cognitive radio would [21]. Specifically, as the cognitive radio utilizes different portions of the frequency spectrum over time, the localization scheme must account for frequency mobility to continue position estimation. When spatial mobility is additionally considered, the problem extends beyond what standard localization techniques can offer. Therefore, source localization of a cognitive radio demands some level of adaptation in the localization process to accurately estimate position [21]. One potential solution to this problem is semi-range based localization.

3. Semi-Range Based Localization Schemes

Semi-range based localization has recently been proposed for primary user source localization via a cognitive radio network [5], [17]. Positioning information about the primary users is essential to identify which frequency bands are available for use and to prevent interference between the secondary user and primary user networks [5]. In this scenario, the secondary users act as a wireless RF sensor network by performing spectrum sensing to identify unused portions of the frequency spectrum for opportunistic usage [5], [17]. The positions of the primary users are determined using only the local spectrum sensing decisions from the secondary user network [5], [17]. In this way, frequency awareness is maintained throughout the localization scheme, which is also a

desirable property for source localization of a cognitive radio. The central idea behind semi range-based localization is exploiting the relationship between the distance of the secondary user to the primary user and the probability of the secondary user detecting the primary user [5], [17]. Thus, spatial awareness is also inherent in semi-range based localization. Given these two characteristics, semi-range based localization is extended in this thesis for cognitive radio source localization using a wireless RF sensor network.

a. Semi-Range Based Iterative Localization Algorithm (ISRB)

Semi-range based localization was originally introduced by Ma et al. [5]. Their distinct contribution is the introduction of a hybrid localization algorithm that takes advantage of key features from both range-based and range-free localization schemes in a cognitive radio environment. This is accomplished in two ways. First, the local binary spectrum sensing decisions of all secondary users in range of one specific primary user are used to estimate the probability of detection at all secondary users. All positions of the secondary users are assumed to be known in advance as each secondary user acts as an anchor node to calculate the final position estimate. Second, the probability of detection is used to estimate the distance from each secondary user to the primary user similar to the way range-based schemes utilize a specific metric to estimate point-to-point distance. In these two ways, Ma's localization algorithm behaves in a range-based as well as range-free manner. Therefore, because of its hybrid nature, Ma et al. have appropriately entitled their technique a semi-range based iterative localization algorithm (ISRB). [5]

b. Practical Semi-Range Based Localization Algorithm (PSRB)

One shortfall of ISRB is the requirement for advance knowledge of the primary user's transmission power given that one of the fundamental goals of a cognitive radio is no explicit cooperation from the primary user of that frequency spectrum [5], [17]. As such, there can be no expectation of knowing the primary user's exact transmission power in advance [17]. Wang et al. has sought to correct this deficiency by proposing a practical semi range-based localization algorithm (PSRB) which does not require the primary user's transmission power to be known in advance [17]. Rather, it

becomes an additional parameter to be estimated during the localization process [17]. This is accomplished by approximating the primary user's power through the iterative non-linear least squares method (NLSM) [17]. However, both ISRB and PSRB rely on the local binary spectrum sensing decisions obtained by the secondary users in the cognitive radio network.

C. APPLICATION AREA OF COGNITIVE RADIO, SPECTRUM SENSING, AND LOCALIZATION IN WIRELESS SENSOR NETWORKS: IEEE STANDARD 802.22 – WIRELESS REGIONAL AREA NETWORKS (WRAN)

The most immediate application of cognitive radio technology comes from the IEEE 802.22 Working Group (WG), which aims to provide last mile rural broadband wireless access through Wireless Regional Area Networks (WRAN) operating in television (TV) white spaces [1], [19], [20]. Completed earlier this year, the IEEE 802.22 WRAN standard employs cognitive radio technology in an unlicensed fashion on top of legacy TV broadcasting networks [1], [19], [20]. As such, the cognitive radio network cannot interfere with the operation of the existing legacy TV broadcast network [1], [19], [20]. Having rights to the allocated spectrum, those radios within the legacy TV broadcast network are identified as primary users [1], [3], [5], [19], [20]. Those cognitive radios operating within the WRAN are secondary users because they have limited or no rights to the allocated spectrum and must perform spectrum sensing to prevent incumbent interference [1], [3], [5], [19], [20]. It is important to note that the 802.22 WG is not alone in their ambition for the development of cognitive radio technologies [20]. Multiple other technologies, such as IEEE standard 802.11af for wireless local area networks in the TV whitespaces [20], are also being developed to take advantage of cognitive radio.

The network topology of the IEEE 802.22 WRAN is shown in Figure 4 [28]. The 802.22 WRAN is a point-to-multipoint system where a single base station (BS) manages all consumer premise equipment (CPE) within its cell [1], [19]. The average cell is intended to cover a 33 kilometer radius but may extend up to 100 kilometers if power is not restricted [1], [19]. A maximum of 255 CPEs are supported per BS per TV channel

[1]. The BS controls medium access and communicates in the downstream direction to all CPE, while the CPE respond in the upstream direction to the BS [1], [19]. The 802.22 physical (PHY) layer is based on orthogonal frequency-division multiple access (OFDMA) with support for data rates of 1.5 Mbps in the downstream direction and 384 kbps upstream [1], [19]. To facilitate medium access control (MAC), a superframe structure is introduced at the MAC layer as shown in Figure 5 [1]. Superframes are used to facilitate incumbent protection, synchronization with adjacent 802.22 WRAN cells, and self-coexistence [1], [19]. Such actions are coordinated through superframe control headers (SCH) and MAC frame control headers (FCH) at the beginning of each frame [1], [19]. One superframe consists of 16 MAC frames, which are further divided into downstream and upstream sub-frames [1], [19]. The duration of one MAC frame is 10 milliseconds, which implies that one superframe lasts 160 milliseconds [1].

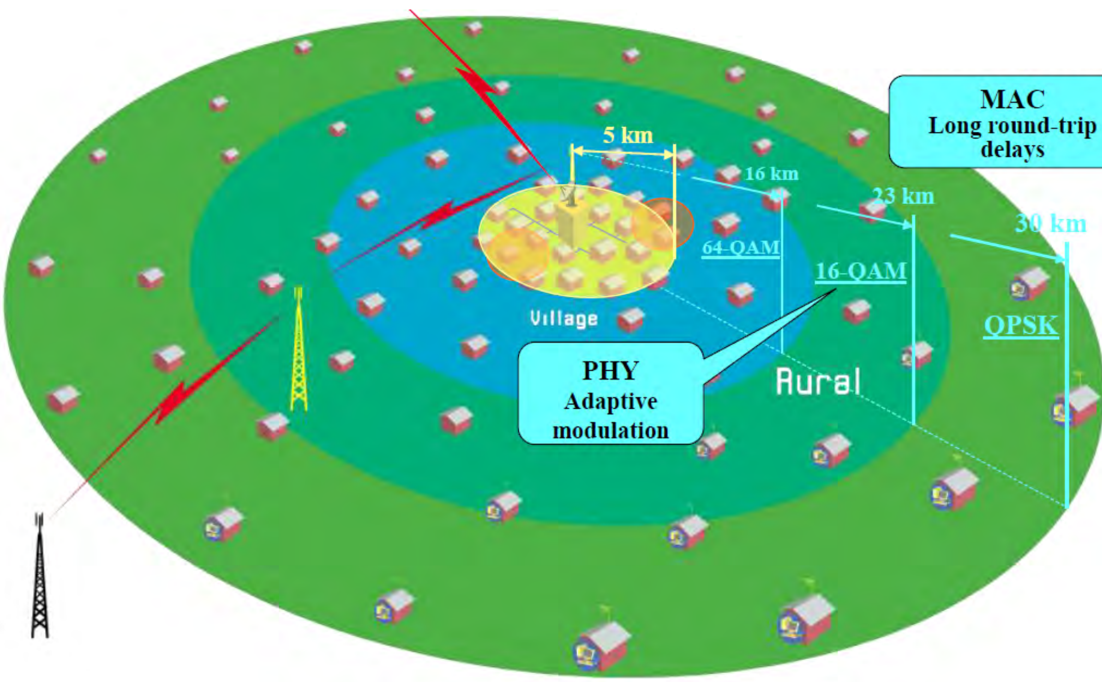

Figure 4. IEEE 802.22 WRAN topology (From [28]).

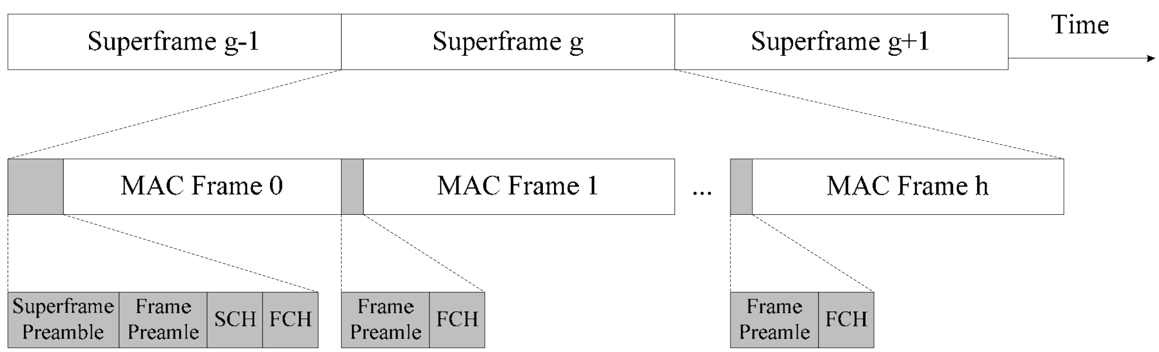

Figure 5. IEEE 802.22 MAC and superframe structure (From [1]).

Spectral awareness in IEEE 802.22 is gained through TV channel usage database access and spectrum sensing [29]. Spectrum sensing is performed in a cooperative distributed manner and is controlled by the base station [1], [19]. In the SCH, designated quiet periods (QP) are established within a superframe where no transmission by the CPE is authorized [1], [19]. Rather, the BS directs any or all CPE to perform spectrum sensing in various TV channels of interest to identify the presence or absence of primary users [1], [19]. QP can take place within a MAC frame (i.e., intra-frame QP) for fast sensing or between MAC frames (i.e., inter-frame QP) for fine sensing as depicted in Figure 6 [1], [19]. Fast sensing is conducted very quickly (e.g., less than 1 millisecond per channel) to be extremely efficient [1], [19]. Based on the results of fast sensing, the BS may direct fine sensing as needed to develop more detailed measurements [1], [19]. During fine sensing, alternative spectrum sensing methods other than energy detection are used, potentially lasting on the order of a few milliseconds [1], [19].

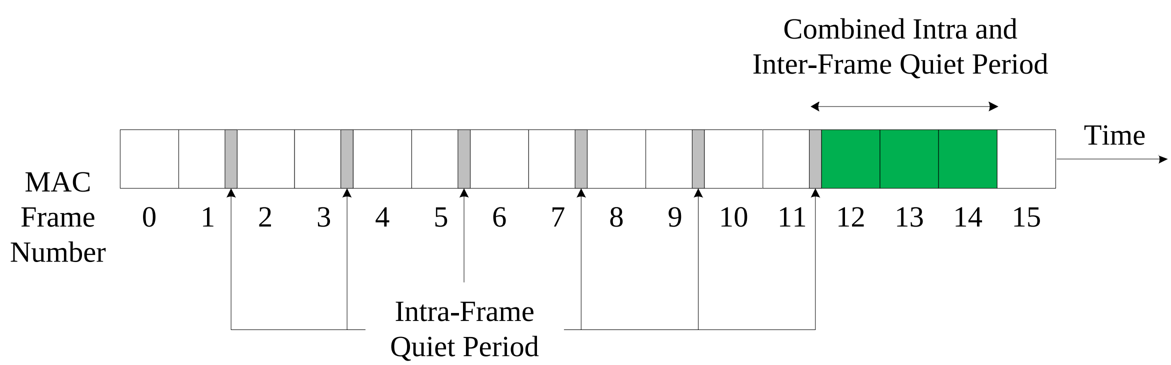

Figure 6. IEEE 802.22 intra-frame and inter-frame quiet periods (From [1]).

Localization is performed through both geo-location database access and satellite-based geo-location technology (e.g., Global Positioning System (GPS), Galileo, etc.) in the IEEE 802.22 standard [29]. The former is used to verify the presence and channel occupancy of the primary users, while the latter is used for self-location among the BS and CPEs [29]. All BSs and CPEs are required to know their position before any transmission can occur [29]. Since positioning information, spectrum sensing, and channel usage database access drive interference prevention, spatial awareness is central to enabling cognitive functionality in the 802.22 standard [29].

An overview of spectrum sensing methods and localization using a wireless RF sensor network was presented in this chapter. An application area was also presented to illustrate how these concepts fit together in the context of cognitive radio and cognitive radio networking. These ideas are built upon and extended to solve the problem of cognitive radio source localization in Chapter III. The proposed extended semi range-based localization scheme is presented in detail.

III. EXTENDED SEMI RANGE-BASED (ESRB) LOCALIZATION SCHEME FOR COGNITIVE RADIO POSITIONING

An overview of spectrum sensing and localization in wireless RF sensor networks was presented in Chapter II. Specifically, the semi-range based localization algorithm was introduced to illustrate how a wireless RF sensor network can be used to determine the location of an emitter of interest in a single frequency band using spectrum sensing as shown in Figure 1 [5], [17]. The ideas previously presented are extended to the problem of source localization of a cognitive radio using multiple frequency bands in this chapter. An in depth explanation of the proposed ESRB localization scheme is provided to accomplish this task. Four fundamental aspects of the scheme are examined: 1) cooperative spectrum sensing, 2) spectral environment mapping, 3) localization through the iterative NLSM, and 4) position refinement.

A. PROPOSED ESRB LOCALIZATION SCHEME

A conceptual diagram of the proposed ESRB localization scheme is shown in Figure 7. Each block represents a specific function of the ESRB localization scheme. The italicized phrases within each block represent what element is responsible for performing the function and where the function takes place in the environment. The text over each arrow represents either the information exchanged between two functions or a brief procedural summary of the actions taking place between sub-functions. The breakdown of each function shown in Figure 7 is discussed below.

Spectrum sensing describes an energy detection process where a determination is made as to whether or not a user is occupying a specific band of the frequency spectrum (i.e., a channel). Spectral environment mapping involves interpretation of the spectral scanning results from the wireless sensor network to build an occupancy map of the environment's frequency usage (i.e., which channels are occupied and which are not). Localization estimates the position of a user within an occupied channel. Lastly, position refinement encompasses evaluation and addition of potential secondary users discovered in the environment and recalculation of previous position estimates using new

measurement data. The proposed ESRB localization scheme utilizes *n*-bit spectrum sensing at the wireless sensor nodes [18], the majority rule [17], [23] for global decision making during spectral environment mapping at the decision maker, and semi range-based localization [5], [17] in the localization and position refinement processes at the decision maker.

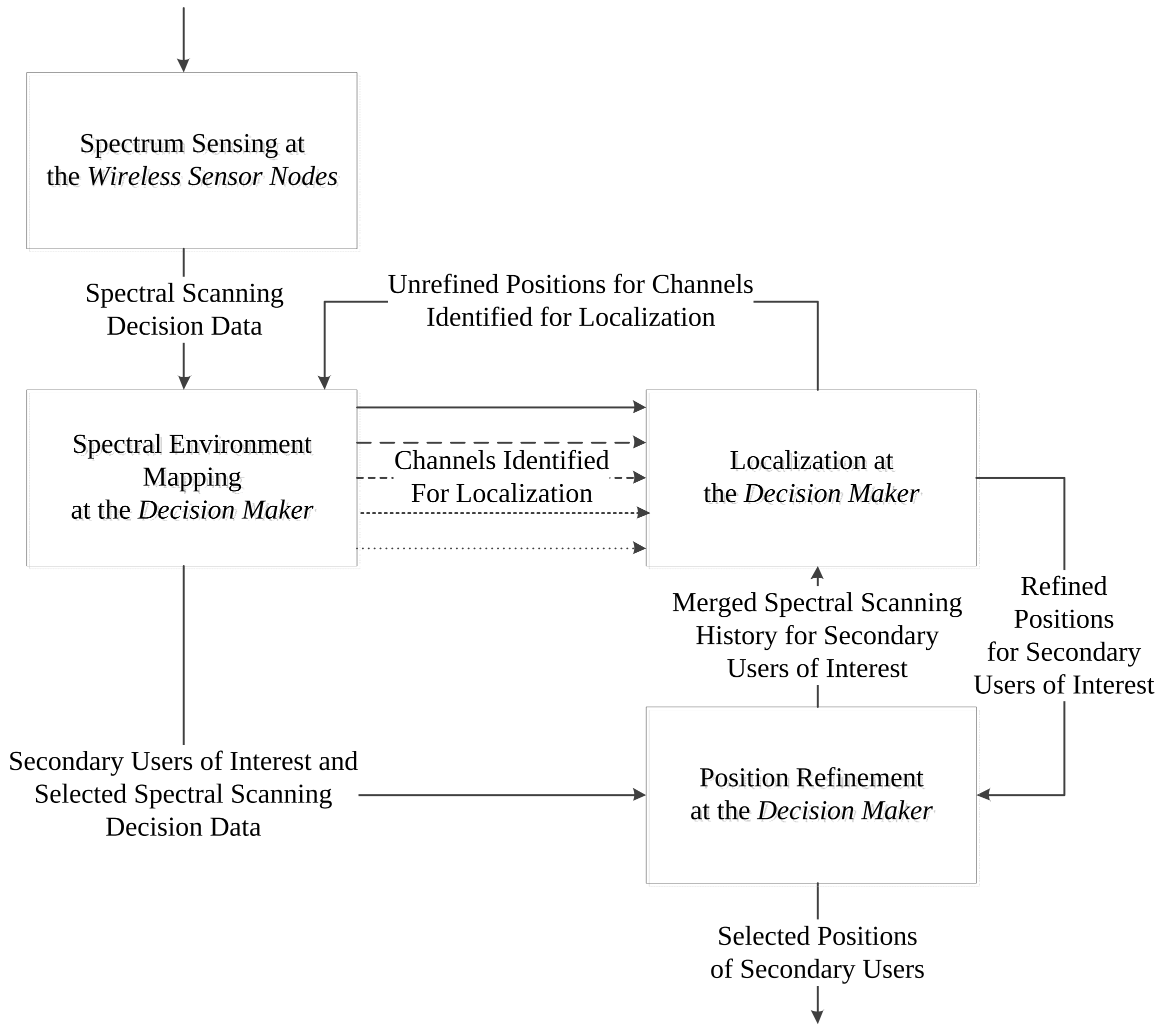

Figure 7. Conceptual diagram of the proposed extended semi range-based (ESRB) localization scheme for cognitive radio positioning.

The execution of the ESRB localization scheme begins with spectrum sensing at the wireless sensor nodes in the wireless sensor network. Each sensor node examines a fixed portion of bandwidth (i.e., a channel) of the entire frequency spectrum of interest (i.e., all channels) over a fixed interval of time and records the presence or absence of a

user. After examining a single channel, the sensor node moves to an adjacent channel and performs spectrum sensing once again. After the entire spectrum of interest is examined, a sensor node has completed one spectral scan. All sensor nodes then report their spectral scanning results to a single decision maker for processing and repeat the spectral scanning process indefinitely.

The decision maker in turn begins to aggregate the spectral scanning results of the entire wireless sensor network in order to make a global decision in regards to the occupancy of the frequency spectrum. This process is called spectral environment mapping because a map of the environment's channel occupancy can be created as time progresses and more spectral scanning results become available. From this map, the decision maker can understand which portions of the frequency spectrum are occupied and which are not. For those channels that are occupied, the decision maker hastily localizes the user in the channel. These unrefined position estimates are then fed back into the spectral environment mapping process where a decision is made as to whether a primary or secondary user is occupying that channel. To discriminate between which estimated positions are primary or secondary users, the decision maker references a geo-location database of primary users located within the environment. The assumption is made that the decision maker has access to the same primary user geo-location database as the secondary user network has access to, such as in the IEEE 802.22 standard [30–32].

Once the decision maker has completed user discrimination of all occupied channels, those users of interest, along with their recorded measurements and estimates (e.g., estimated position, estimated transmission power, channel occupied, etc.), are stored in memory to develop a history of secondary user activity. As new spectral scans become available, the decision maker references this history to cross-reference newly discovered positions of potential secondary users with positions previously found. If a match is identified within an acceptable level of tolerance, the previous spectral scanning results contained in memory are merged with the latest spectral scanning results. The updated spectral scanning history is then fed back into the localization process to refine the position estimate of all potential secondary users discovered. Finally, the decision

maker screens the refined positions against the primary user geo-location database again to confirm the refined positions are not those of primary users. Those secondary user position estimates, which have been validated for more than one localization iteration, are declared to be secondary users. If the secondary user moves during ESRB localization scheme, the decision maker will record the estimated positions of the mobile secondary user after each localization attempt.

The subsequent sections provide greater detail of the methods used to facilitate execution of the ESRB localization scheme.

B. COOPERATIVE SPECTRUM SENSING IN THE ESRB LOCALIZATION SCHEME

The incorporation of cooperative spectrum sensing in the ESRB localization scheme is shown in Figure 8. The dashed box symbolizes the single box used in Figure 7 to describe the overall cooperative spectrum sensing function. Each of the boxes inside the dashed box symbolizes sub-functions of the cooperative spectrum sensing function. The single boxes outside the dashed box indicate the summary function blocks from Figure 7 which interact with the cooperative spectrum sensing sub-functions. The text over each arrow continues to represent either the information exchanged between functions or a brief procedural summary of the actions taking place between sub-functions.

Each of the sensor nodes within the wireless RF sensor network performs energy detection in a fixed bandwidth *W* (i.e., channel *k*) over a time interval *T* [5], [17], [23] with the intent of deciding between two hypotheses [5], [17], [23]

$$x_i^{(k)}(t) = \begin{cases} n(t), & H_0 \\ s_i^{(k)}(t) + n(t), & H_1 \end{cases}, \qquad 0 < t \le T \tag{4}$$

where $x_i^{(k)}(t)$ is the observed signal at the *i*th sensor node in channel *k*, $s_i^{(k)}(t)$ is the signal of interest at the *i*th sensor node in channel *k*, and $n(t)$ is bandlimited additive white Gaussian noise (AWGN) with zero mean and variance of σ_0^2 [17]. The channel is assumed to be time-invariant during the spectrum sensing process [5], [17], [23].

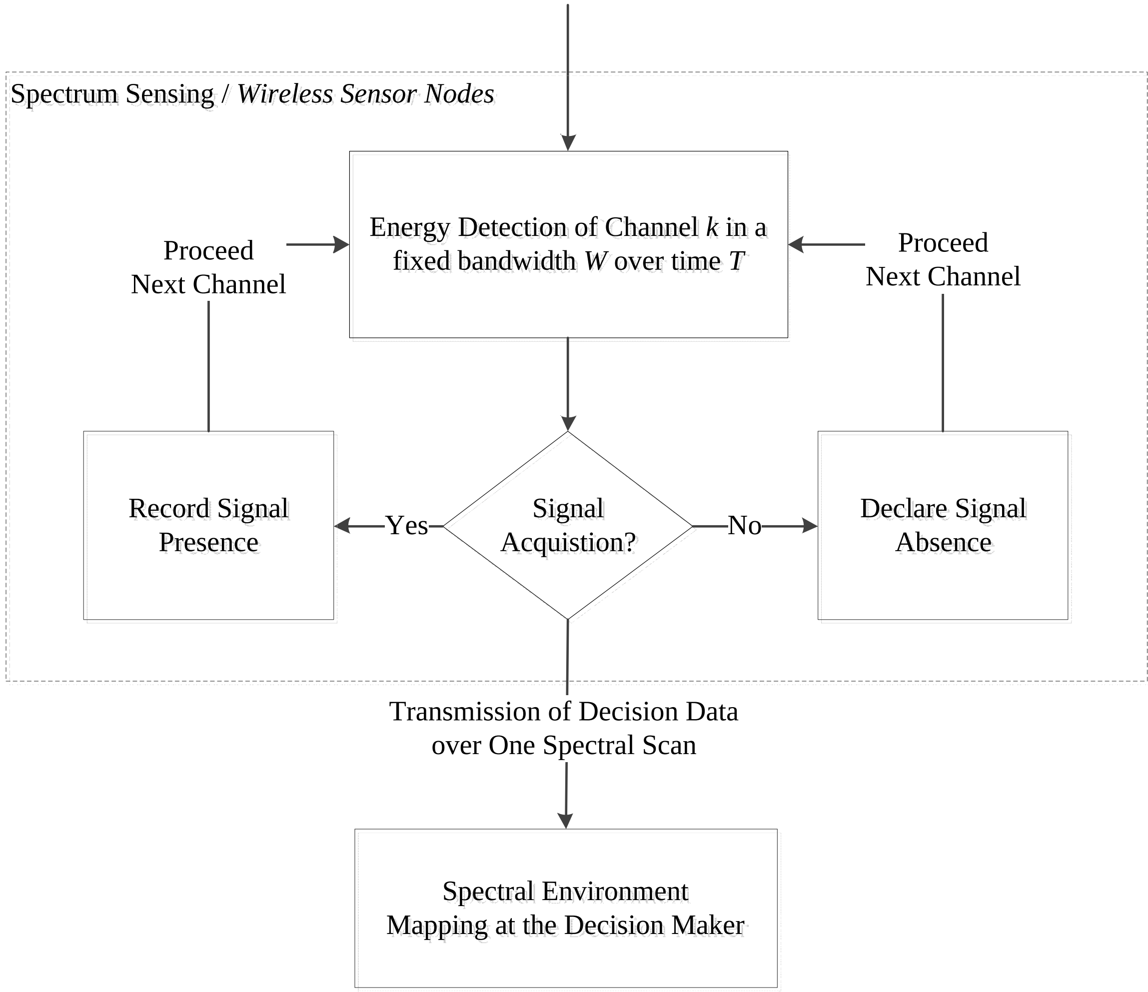

Figure 8. Detailed conceptual diagram of cooperative spectrum sensing in the proposed ESRB localization scheme for cognitive radio positioning.

To account for multipath fading and path loss in the environment, the instantaneous received signal power is modeled as a Rayleigh random variable, while the average signal power is inversely proportional to distance raised to a power [5], [17], [23]. Thus, at time *t*, the probability density function (PDF) of the amplitude $s_i^{(k)}(t)$ of the received signal of interest is [17]

$$p_i^{(k)}\left(s_i^{(k)}(t)\right) = \frac{s_i^{(k)}(t)}{\overline{p_i^{(k)}}} \exp\left(-\frac{\left(s_i^{(k)}(t)\right)^2}{2\overline{p_i^{(k)}}}\right) \tag{5}$$

where

$$\overline{p_i^{(k)}} = cP_{tx}^{(k)}\left(d_i^{(k)}\right)^{-\alpha} \tag{6}$$

is the average power of the received user signal at the *i*th sensor node in channel *k*. The distance between the user occupying channel *k* and the *i*th sensor node is represented by $d_i^{(k)}$, the transmission power of the user occupying channel *k* is represented by $P_{tx}^{(k)}$, the scalar *c* is a constant which encompasses all else which can influence the received signal power (e.g., antenna gains, antenna heights, etc.), and α is the path loss factor [17]. The assumption is made that all other factors encompassed in the constant *c* are identical for all receivers (e.g. antenna heights, etc.) and that all antenna gains are approximated as independent of direction. When the occupying user's signal is present in channel *k*, the instantaneous SNR at the *i*th sensor node is given by [17]

$$\gamma_i^{(k)} = \frac{\left(s_i^{(k)}\right)^2}{\sigma_0^2} \tag{7}$$

which is an exponential random variable [17]. Therefore, the average SNR is [17]

$$\begin{aligned}\overline{\gamma_i^{(k)}} &= \frac{\overline{\left(s_i^{(k)}\right)^2}}{\sigma_0^2} \\ &= \frac{cP_{tx}^{(k)}\left(d_i^{(k)}\right)^{-\alpha}}{\sigma_0^2}\end{aligned} \tag{8}$$

The energy collected over the sensing period *T* in the bandwidth *W* at the *i*th sensor node in channel *k* is designated as $X_i^{(k)}$ and has the distribution [5], [17], [23]

$$X_i^{(k)} \approx \begin{cases} \chi_{2u}^2, & H_0 \\ \chi_{2u}^2\left(2\gamma_i^{(k)}\right), & H_1 \end{cases} \tag{9}$$

where $u = TW$ is the time-bandwidth product, χ_{2u}^2 is the central chi-square distribution with 2*u* degrees of freedom, and $\chi_{2u}^{2u}\left(2\gamma_i^{(k)}\right)$ is the non-central chi-square distribution with 2*u* degrees of freedom and non-centrality parameter $2\gamma_i^{(k)}$ [5], [17], [23].

The average probability of false alarm $\overline{P_{f,i}^{(k)}}$ over a Rayleigh fading channel at the *i*th sensor node in channel *k* is given by [5], [17], [23]

$$\overline{P_{f,i}^{(k)}} = E\left[P\left\{ X_i^{(k)} > \lambda_i \mid H_0 \right\} \right] = \frac{\Gamma\left(u, \frac{\lambda_i}{2} \right)}{\Gamma(u)} \tag{10}$$

where λ_i is the energy detection threshold at the ith sensor node, $\Gamma(\cdot)$ is the gamma function, and $\Gamma(\cdot,\cdot)$ is the incomplete gamma function. The average probability of detection $\overline{P_{d,i}^{(k)}}$ is given by [5], [17]

$$\overline{P_{d,i}^{(k)}} = E\left[P\left\{ X_i^{(k)} > \lambda_i \mid H_1 \right\} \right] = e^{-\frac{\lambda_i}{2}} \sum_{n=0}^{u-2} \frac{1}{n!}\left(\frac{\lambda_i}{2} \right)^n + \left(\frac{1+\overline{\gamma_i^{(k)}}}{\overline{\gamma_i^{(k)}}} \right)^{u-1} \left[e^{-\frac{\lambda_i}{2\left(1+\overline{\gamma_i^{(k)}}\right)}} - e^{-\frac{\lambda_i}{2}} \sum_{n=0}^{u-2} \frac{1}{n!} \left(\frac{\lambda_i \overline{\gamma_i^{(k)}}}{2\left(1+\overline{\gamma_i^{(k)}}\right)} \right)^n \right]. \tag{11}$$

For the purposes of the ESRB localization scheme, the desired $\overline{P_{f,i}^{(k)}}$ is declared in advance as a performance requirement for each sensor node. Furthermore, it is held constant for all sensor nodes in all channels [5], [17]. Therefore, given a universal desired $\overline{P_f}$ and a specified time-bandwidth product u, the energy detection threshold λ_i is determined using (10) [5], [17]. Furthermore, since all nodes are assigned the same $\overline{P_f}$, they all have the same λ [5], [17]. Finally, with u and λ pre-determined, $\overline{P_{d,i}^{(k)}}$ can be considered solely a function of $\overline{\gamma_i^{(k)}}$ [5], [17].

After the received signal energy is compared against the energy detection threshold of the sensor node, a decision is made with regards to the presence or absence of a user, and the result is recorded as a binary one or zero, respectively [5], [17]. Each sensor node then observes the adjacent channel and repeats the spectrum sensing procedure. After all channels have been examined, each node reports their 1-bit spectrum sensing results as a single row vector (i.e., a spectral scan) to the decision maker [5], [17].

C. SPECTRAL ENVIRONMENT MAPPING IN THE ESRB LOCALIZATION SCHEME

The incorporation of spectral environment mapping in the ESRB localization scheme is shown in Figure 9. Spectral environment mapping takes places at the decision maker where additional computational resources are assumed available. The goal of the spectral environment mapping function is to fuse all decision data from the wireless sensor network to create an overall map of the spectral environment. From this map, a decision can be made as to whether a secondary user exists in the environment and which channel it is occupying. The function consists of four sub-functions: 1) decision aggregation, 2) decision refinement, 3) channel identification for localization, and 4) position comparison and user identification.

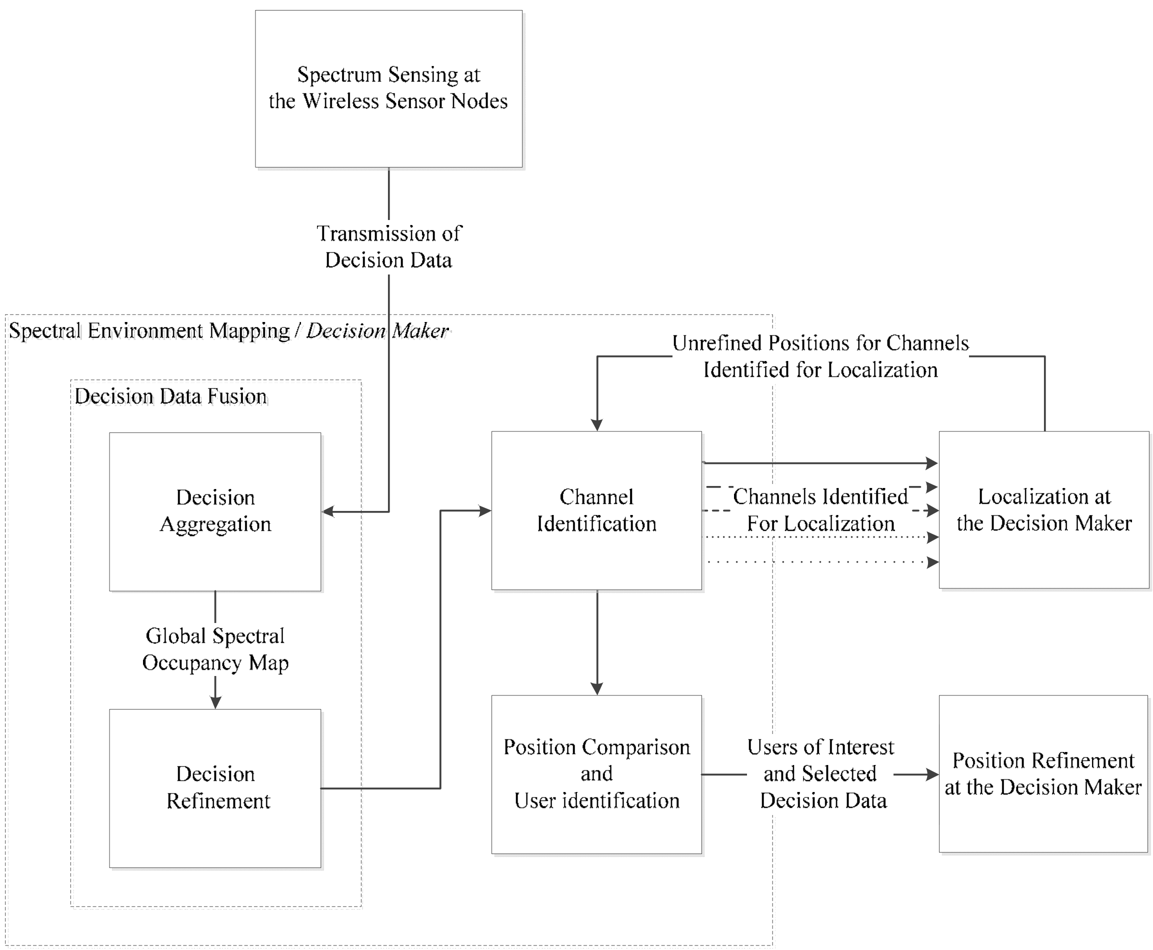

Figure 9. Detailed conceptual diagram of spectral environment mapping in the proposed ESRB localization scheme for cognitive radio positioning.

1. Decision Data Fusion

Spectral environment mapping begins once the decision maker has collected N_P spectral scans from the sensor network [17]. Under the decision aggregation sub-function, the collected spectral scans at the decision maker are organized as a three-dimensional tensor

$$\mathbf{Z} = \left[z_{ijk} \right]_{N \times N_P \times K} \tag{12}$$

where N is the number of sensor nodes, N_P is the number of spectral scans, K is the total number of channels examined, and

$$z_{ijk} = \begin{cases} 0 & H_0 \\ 1 & H_1 \end{cases} \tag{13}$$

represents the local spectrum sensing decision at the ith sensor node from the jth spectral scan of channel k [17]. The user occupancy within each channel is assumed to be independent of one another. Therefore, the decision maker breaks down the collected spectral scanning decisions on a per channel basis to perform data fusion. Thus, for a single channel k, (12) is reduced to a two-dimensional matrix [17]

$$\mathbf{X}^{(k)} = \left[x_{ij}^{(k)} \right]_{N \times N_P} \tag{14}$$

and (13) is reduced to [17]

$$x_{ij}^{(k)} = \begin{cases} 0 & H_0 \\ 1 & H_1 \end{cases}. \tag{15}$$

Data fusion is performed using the majority decision rule which is shown in [23] to optimize the sensor network's detection performance when $\overline{P_{d,i}}$ and $\overline{P_{f,i}}$ have the same order. That is, if more than $N/2$ nodes indicate the channel is occupied, the user is declared present. Applying this rule to $\mathbf{X}^{(k)}$, a global decision is acquired for channel k [17]

$$\mathbf{y}^{(k)} = \left[y_j^{(k)} \right]_{1 \times N_P} \tag{16}$$

where $y_j^{(k)}$ is the data fusion result of the jth spectral scan. From the global decision vector $\mathbf{y}^{(k)}$, a two-dimensional decision matrix is formed for channel k [17]

$$\mathbf{Y}_{\mathbf{M}}^{(k)} = \operatorname{diag}\left[y_1^{(k)}, y_2^{(k)}, \ldots, y_{N_P}^{(k)} \right] \tag{17}$$

which is used by the measurement refinement sub-function to filter the spectral scanning results by the following operation [17]

$$\begin{aligned} \tilde{\mathbf{X}}^{(k)} &= \mathbf{X}^{(k)} \mathbf{Y}_{\mathbf{M}}^{(k)} \\ &\triangleq \left[\tilde{x}_{ij}^{(k)} \right]_{N \times N_P} . \end{aligned} \tag{18}$$

This same process is applied to all channels to develop a complete global spectral occupancy map.

2. Using Position Estimation to Establish User Identity

The completed map indicates occupied channels and where white space exists over N_P spectral scans, but it does not indicate which type of user is present in the occupied channels. To answer this question, the decision maker localizes the users in all channels which are occupied. The central idea is that the decision maker uses the position information from the spatial domain to establish user identity in the frequency domain. This process is accomplished by the channel identification sub-function, which utilizes the localization function to develop an unrefined position estimate. Accuracy of the position estimate increases when the number of spectral scans increases (see Chapter IV.C.2). Those unrefined position estimates from the localization process are used to establish user identity through the position comparison sub-function.

Given the coarse positions of all users in occupied channels, the position comparison sub-function accesses a primary user database to determine which unrefined positions match known primary users' positions within a level of tolerance. An error tolerance radius is defined around the true positions of the primary users gleaned from the database. If a position estimate falls within the tolerance radius of a true primary user's position, then the hastily localized user is declared to be a primary user. If a position estimate does not match any primary user, the user becomes a user of interest as it may be a secondary user. For all users of interest identified, their position estimates, channel occupancy, and associated spectral scanning decision data from the sensor network are

stored in memory at the decision maker and passed to the position refinement function. In this way position estimation is used to establish user identity.

D. LOCALIZATION THROUGH THE ITERATIVE NON-LINEAR LEAST SQUARES METHOD IN THE ESRB LOCALIZATION SCHEME

The incorporation of localization through the iterative non-linear least squares method in the ESRB localization scheme is shown in Figure 10. The localization function occurs at the decision maker. Each time the localization function is invoked, the localization function determines the position of one user occupying one channel. The spectral environment mapping function utilizes the unrefined position results of the localization function to distinguish between primary or secondary users in the environment. As such, multiple localization attempts are made. This is symbolized by multiple arrows leading into the detailed localization function block. The position refinement function utilizes the localization function to increase the accuracy of the position estimates for probable secondary users. Localization is accomplished in four steps: 1) estimation of the probabilities of detection for all sensor nodes in channel *k*, 2) conversion of the probabilities of detection estimates into SNR estimates, 3) conversion of the SNR estimates into distances, and 4) position estimation using the NLSM.

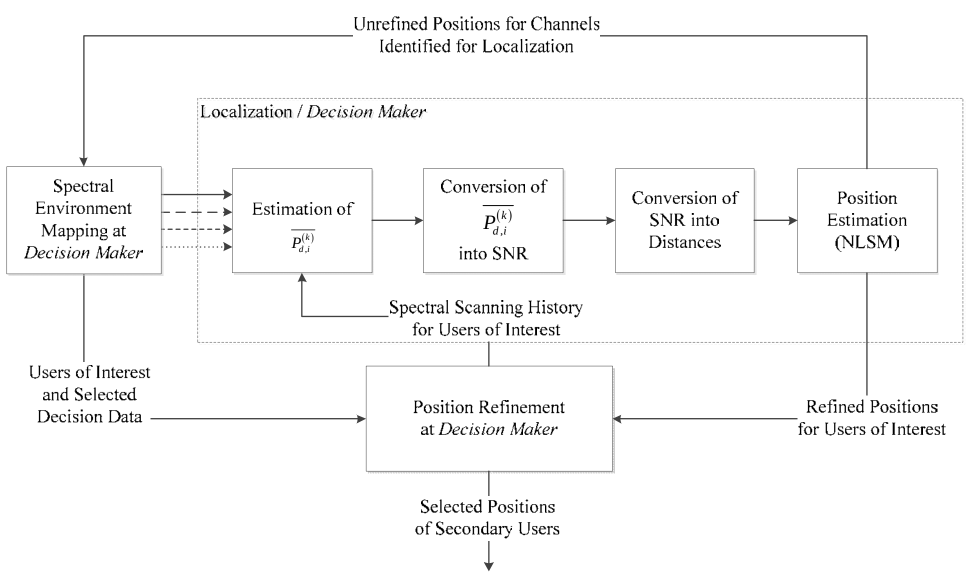

Figure 10. Detailed conceptual diagram of localization through the iterative non-linear least squares method (NLSM) in the proposed ESRB localization scheme for cognitive radio positioning.

1. Average SNR Estimation Through the Probability of Detection Estimates

From $\hat{\mathbf{X}}^{(k)}$, an estimate of the average probability of detection at the *i*th sensor node of the user occupying channel *k* is obtained as

$$\overline{P_{d,i}^{(k)}} = \frac{\sum_{j=1}^{T_P} x_{ij}^{(k)}}{\mathrm{tr}\left(\mathbf{Y}_{\mathbf{M}}^{(k)}\right)} \quad (19)$$

As in the ISRB [5] and PSRB [17] localization algorithms, the estimate of $\overline{P_{d,i}^{(k)}}$ is used to obtain $\overline{\gamma_i^{(k)}}$ by (11); however, $\overline{\gamma_i^{(k)}}$ cannot be directly obtained from (11) due to its complexity [5], [17]. Instead, a table lookup method is used to solve for $\overline{\gamma_i^{(k)}}$ given the estimate of $\overline{P_{d,i}^{(k)}}$. Tables of $\overline{\gamma_i^{(k)}}$ for various values of *u* and λ are generated and stored in memory at the decision maker so that, given a specific pair of values for *u* and λ, the correct $\overline{\gamma_i^{(k)}}$ is obtained within the level of tolerance of the table calculations [5], [17]. The assumption is made that the decision maker has enough memory and computational resources to perform such an operation [17].

2. Position and Power Estimation Through the Average SNR Estimates and the Iterative Non-Linear Least Squares Method

The value of the SNR estimate $\overline{\gamma_i^{(k)}}$ is the relationship between the distance of the sensor node from the user occupying channel *k* and the SNR at the sensor node [5], [17]. In general, the farther the sensor node is away from the user occupying the channel, the lower the SNR will be at the sensor node [5], [17]. This relationship is illustrated by (8), where the distance of the occupying user $d_i^{(k)}$ can be solved for directly from the SNR estimate $\overline{\gamma_i^{(k)}}$. However, to accomplish this, the transmission power of the occupying user $P_{tx}^{(k)}$, the noise variance σ_0^2, the path loss factor α, and the constant *c* must be known in advance. Even when precise values for these parameters are not known in advance, the overall localization process is capable of handling such inaccuracies as

demonstrated through simulation in [5]. This is possible because of adequate spatial separation amongst the sensor nodes and resiliency in the estimation process through collaborative spectrum sensing [5].

As mentioned in Chapter II.B.3.b, the motivation behind the PSRB localization algorithm is to remove any requirement for cooperation between the secondary user network and the primary user network in the localization process [17]. As such, $P_{tx}^{(k)}$ becomes an additional parameter to be estimated. It is assumed to be unavailable due to lack of cooperation between networks [17]. This assumption is carried forward into the ESRB localization scheme, where the position and transmission power of the secondary user are parameters estimated by the sensor network. No cooperation is assumed between the sensor network and the primary or secondary user networks.

A two-dimensional Cartesian coordinate system is used to establish true positions for all elements in the environment with the decision maker located at the origin [17]. This arrangement is shown in Figure 11. The true position and power of the user occupying channel *k* is represented by a row vector [17]

$$\theta^{(k)} = \left[x^{(k)}, y^{(k)}, P_{tx}^{(k)} \right] \tag{20}$$

where $x^{(k)}$ and $y^{(k)}$ are the Cartesian position coordinates of the user occupying channel *k*, and $P_{tx}^{(k)}$ is the transmission power of the user occupying channel *k* [17]. Similarly, for the *i*th sensor node, its Cartesian coordinates are represented as $\left(a_i, b_i\right)$ where a_i is the horizontal Cartesian coordinate and b_i is the vertical Cartesian coordinate [17].

To solve for the true position of the user occupying channel *k* using the spectral scanning decision data available, (8) is rewritten as [17]

$$\left(d^{(k)}\right)^2 - \left(\frac{cP_{tx}^{(k)}}{\overline{\overline{\gamma_i^{(k)}}} \times n_0^2} \right)^{\frac{2}{\alpha}} = 0 \tag{21}$$

which, for the *i*th sensor node, is further expanded to [17]

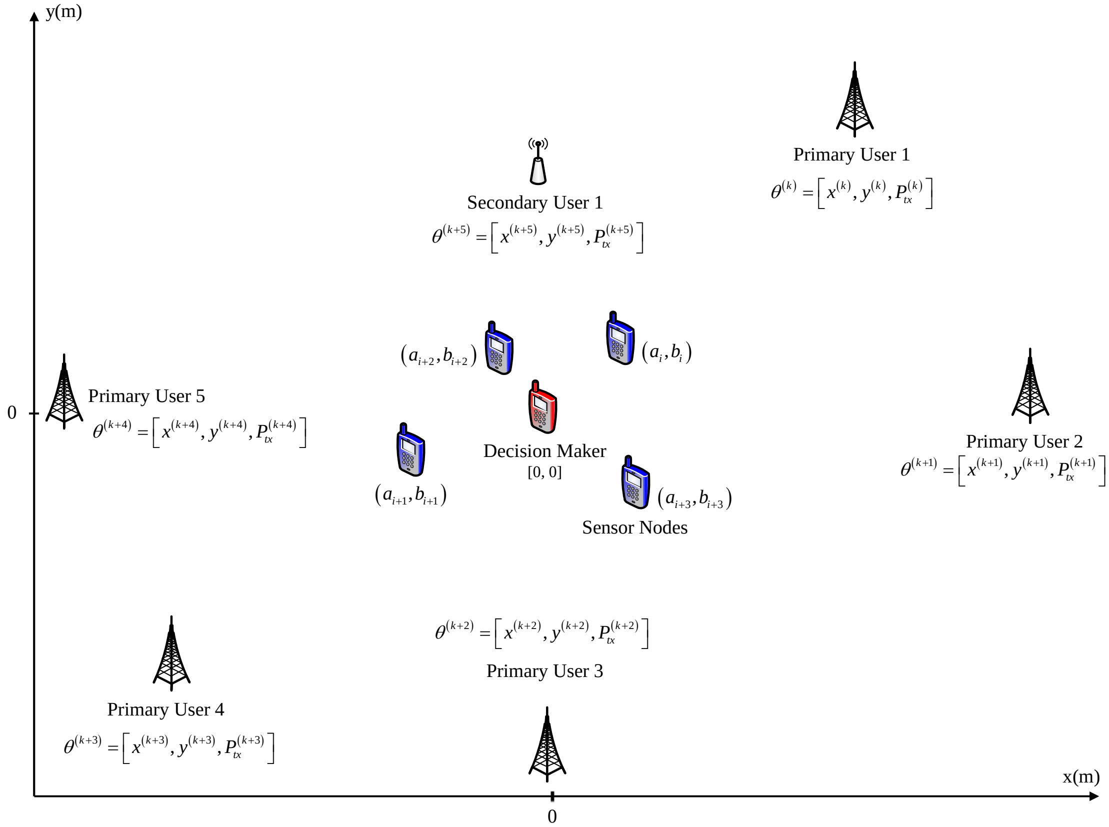

Figure 11. Two-dimensional Cartesian coordinate system of the environment in the ESRB localization scheme.

$$\left(x^{(k)}\right)^2 - 2a_i x^{(k)} + \left(y^{(k)}\right)^2 - 2b_i y^{(k)} + a_i^2 + b_i^2 - \left(\frac{c}{\overline{\gamma_i^{(k)}} \times n_0^2}\right)^{\frac{2}{\alpha}} \times \left(P_{tx}^{(k)}\right)^{\frac{2}{\alpha}} = 0 \tag{22}$$

using the fact that the square of distance d between any two points in a Cartesian coordinate system can be expressed as

$$d^2 = \left(x_2 - x_1\right)^2 + \left(y_2 - y_1\right)^2 \tag{23}$$

with the first point located at $\left(x_1, y_1\right)$ and the second point located at $\left(x_2, y_2\right)$. Equation (22) is then rewritten as a function of $\theta^{(k)}$ to aid in developing an estimate of the user's position and power [17]:

$$f_i\left(\theta^{(k)}\right)=\left(x^{(k)}\right)^2-2a_ix^{(k)}+\left(y^{(k)}\right)^2-2b_iy^{(k)}+a_i^2+b_i^2-\left(\frac{c}{\bar{\gamma}_i^{(k)}\times n_0^2}\right)^{\frac{2}{\alpha}}\times\left(P_{tx}^{(k)}\right)^{\frac{2}{\alpha}}. \qquad (24)$$

The estimate of the user's true position and transmit power through the iterative NLSM is defined as

$$\hat{\theta}^{(k)} \triangleq \left[\hat{x}^{(k)},\hat{y}^{(k)},\hat{P}_{tx}^{(k)}\right]. \qquad (25)$$

To achieve the Minimum Mean Square Error (MMSE) of $\hat{\theta}^{(k)}$, the following relationship must be satisfied [17]

$$\sum_{i=1}^{N} f_i^2\left(\hat{\theta}^{(k)}\right)=\min\sum_{i=1}^{N} f_i^2\left(\theta^{(k)}\right). \qquad (26)$$

This can be accomplished through various numerical optimization techniques [33]. Given the overdetermined nature of the system of equations to be solved, where *N* sensor nodes are used to solve for three unknown variables, the iterative non-linear least squares method can provide an optimal local numerical solution [17], [33].

Application of the iterative non-linear least squares method begins by choosing initial values for $\hat{\theta}^{(k)}$ [17], [33]. These initial values are denoted as [17]

$$\hat{\theta}^{(k,0)}=\left(\hat{x}^{(k,0)},\hat{y}^{(k,0)},\hat{P}_{tx}^{(k,0)}\right) \qquad (27)$$

where the superscript (k,l) indicates the *l*th iteration of the non-linear least squares method for the user occupying channel *k*. It is critical that these initial values be as close as possible to the true values in order for the iterative NLSM to converge to a local solution [17], [33]. Locally convergent methods, such as the iterative NLSM, will fail when the initial values are not close to the true solution [33]. Such failures become a significant issue when a small number of spectral scans are available at the decision maker (see Chapter III.C.3 and Chapter IV.C.1). To overcome this drawback, *n*-bit spectrum sensing is incorporated in the cooperative spectrum sensing process of the ESRB localization scheme. Additional logic is also added at the decision maker to overcome failure in any localization attempt.

To develop accurate initial values to seed the iterative NLSM, $P_{tx}^{(k,0)}$ is set to the median transmission power of all secondary and primary users in the environment [17]. The initial Cartesian coordinates $\left(\tilde{x}^{(k,0)}, \tilde{y}^{(k,0)}\right)$ for the user occupying channel k are derived from the sensor node with the highest probability of detection [17]. As in the PSRB localization scheme, the assumption is made that the sensor node with the highest probability of detection lies in the same general direction as the user occupying channel k [17]. To exploit this assumption, sensor node m is assumed closest to the user occupying channel k. Equation (22) can then also be rewritten in polar form as [17]

$$\left(d^{(k,0)}\right)^2 + \left(r_m\right)^2 - 2r_m d^{(k,0)} \cos\left(2\varphi^{(k,0)}\right) - \left(\frac{cP_{tx}^{(k,0)}}{\bar{\gamma}_m^{(k)} \times n_0^2}\right)^{\frac{2}{\alpha}} = 0 \tag{28}$$

where [17]

$$r_m = \sqrt{x_m^2 + y_m^2} \tag{29}$$

and $d^{(k,0)}$ is the initial estimate of the distance between the decision maker at the origin and the occupying user, and $\varphi^{(k,0)}$ is the angle from the decision maker at the origin to sensor node m. The angle $\varphi^{(k,0)}$ is given by [17]

$$\varphi^{(k,0)} = \varphi_m = \begin{cases} \tan^{-1}\left(\dfrac{y_m}{x_m}\right) & x_m > 0 \\ \tan^{-1}\left(\dfrac{y_m}{x_m}\right) + \pi & x_m > 0 \\ \dfrac{\pi}{2} & x_m = 0, y_m \geq 0 \\ -\dfrac{\pi}{2} & x_m = 0, y_m \geq 0 \end{cases} . \tag{30}$$

Solving (28) for $d^{(k,0)}$, we obtain [17]

$$d^{(k,0)} = r_m \cos\left(2\varphi^{(k,0)}\right) + \sqrt{\left(\frac{cP_{tx}^{(k,0)}}{\bar{\gamma}_m^{(k)} \times n_0^2}\right)^{\frac{2}{\alpha}} - \left(r_m\right)^2 \sin^2\left(2\varphi^{(k,0)}\right)} . \tag{31}$$

The initial estimate of the distance between the decision maker at the origin and the occupying user can be translated into initial coordinates $\left(x^{(k,0)}, y^{(k,0)}\right)$ by

$$x^{(k,0)} = d^{(k,0)} \cos\left(\varphi^{(k,0)}\right) \tag{32}$$

$$y^{(k,0)} = d^{(k,0)} \sin\left(\varphi^{(k,0)}\right) \tag{33}$$

.

With $\vec{\theta}^{(k,0)}$ obtained, the first iteration of the non-linear least squares method can begin [17], [33]. Each iteration centers around the relationship given by [17]

$$\vec{\theta}^{(k,l+1)} = \vec{\theta}^{(k,l)} + \kappa \boldsymbol{\psi}^{(k,l)} \tag{34}$$

where $\vec{\theta}^{(k,l)}$ is the current estimate of the position and power of the user occupying channel k, the vector $\boldsymbol{\psi}^{(k,l)}$ contains the Gauss-Newton direction, κ is a scalar which adjusts the magnitude and sign of the Gauss-Newton direction, and $\vec{\theta}^{(k,l+1)}$ is the updated estimate at the end of the iteration. The Gauss-Newton direction $\boldsymbol{\psi}^{(k,l)}$ and the scalar κ provide a correction to the estimate throughout each iteration of the non-linear least squares method [17], [33]. Provided the initial estimate is close to the true solution, the estimate will converge toward the local solution with each correction [17], [33]. In each iteration, the Gauss-Newton direction is obtained by solving the normal equations [17], [33]

$$\left(\mathbf{A}^{(k,l)}\right)^T \mathbf{A}^{(k,l)} \boldsymbol{\psi}^{(k,l)} = -\left(\mathbf{A}^{(k,l)}\right)^T \mathbf{f}^{(k,l)} \tag{35}$$

where [17]

$$\mathbf{f}^{(k,l)} = \left[f_1\left(\vec{\theta}^{(k,l)}\right), f_2\left(\vec{\theta}^{(k,l)}\right), \ldots, f_N\left(\vec{\theta}^{(k,l)}\right)\right]^T \tag{36}$$

and

$$
\mathbf{A}^{(k)} = \begin{pmatrix} \dfrac{\partial f_1\left(\theta^{(k,l)}\right)}{\partial x^{(k)}}, \dfrac{\partial f_1\left(\theta^{(k,l)}\right)}{\partial y^{(k)}}, \dfrac{\partial f_1\left(\theta^{(k,l)}\right)}{\partial P_{tx}^{(k)}} \\ \dfrac{\partial f_2\left(\theta^{(k,l)}\right)}{\partial x^{(k)}}, \dfrac{\partial f_2\left(\theta^{(k,l)}\right)}{\partial y^{(k)}}, \dfrac{\partial f_2\left(\theta^{(k,l)}\right)}{\partial P_{tx}^{(k)}} \\ \vdots \quad\quad \vdots \quad\quad \vdots \\ \dfrac{\partial f_N\left(\theta^{(k,l)}\right)}{\partial x^{(k)}}, \dfrac{\partial f_N\left(\theta^{(k,l)}\right)}{\partial y^{(k)}}, \dfrac{\partial f_N\left(\theta^{(k,l)}\right)}{\partial P_{tx}^{(k)}} \end{pmatrix}
$$

$$
= \begin{pmatrix} 2\left(x^{(k,l)} - a_1\right), 2\left(y^{(k,l)} - b_1\right), -\dfrac{2}{\alpha}\left(\dfrac{c}{\overline{\gamma}_1^{(k)} \times n_0^2}\right)^{\frac{2}{\alpha}} \times \left(P_{tx}^{(k,l)}\right)^{\frac{2-\alpha}{\alpha}} \\ 2\left(x^{(k,l)} - a_2\right), 2\left(y^{(k,l)} - b_2\right), -\dfrac{2}{\alpha}\left(\dfrac{c}{\overline{\gamma}_2^{(k)} \times n_0^2}\right)^{\frac{2}{\alpha}} \times \left(P_{tx}^{(k,l)}\right)^{\frac{2-\alpha}{\alpha}} \\ \vdots \quad\quad \vdots \quad\quad \vdots \\ 2\left(x^{(k,l)} - a_N\right), 2\left(y^{(k,l)} - b_N\right), -\dfrac{2}{\alpha}\left(\dfrac{c}{\overline{\gamma}_N^{(k)} \times n_0^2}\right)^{\frac{2}{\alpha}} \times \left(P_{tx}^{(k,l)}\right)^{\frac{2-\alpha}{\alpha}} \end{pmatrix}. \tag{37}
$$

The scalar κ is found by satisfying [17]

$$
\sum_{i=1}^{N} f_i^2\left(\hat{\theta}^{(k,l+1)}\right) = \min_{\kappa} \sum_{i=1}^{N} f_i^2\left(\hat{\theta}^{(k,l)} + \kappa \boldsymbol{\psi}^{(k,l)}\right). \tag{38}
$$

As iterations proceed, once [17]

$$
\left\| \hat{\theta}^{(k,l+1)} - \hat{\theta}^{(k,l)} \right\| < \varepsilon \tag{39}
$$

is satisfied, where ε is a predefined level of tolerance in the difference between position estimates after each iteration, the iterative method ceases, and $\hat{\theta}^{(k,l+1)}$ is the optimal estimate.

3. Protection Against Divergence Through *n*-bit Spectrum Sensing

As mentioned in Chapter III.C.2, the iterative non-linear least squares method can and will fail when $\hat{\theta}^{(k,0)}$ is not close to the true solution [33]. The failure is due either to the Gauss-Newton direction not being in a direction of descent for $f_i\left(\theta^{(k)}\right)$ or the length

of the Gauss-Newton direction may be too great [33]. This results in an increase of $f_i\left(\theta^{(k)}\right)$ and divergence of the iteration [33]. When this occurs, a solution cannot be obtained from the iterative non-linear least squares method [33].

To help overcome this issue, *n*-bit spectrum sensing is incorporated in the overall ESRB localization scheme to develop accurate initial values as quickly as possible. This is accomplished by modifying the cooperative spectrum sensing process outlined in Chapter III.B. Rather than simply rely on a single bit to indicate the presence or absence of a user, multiple bits are used to indicate how strong the received energy is at the sensor node during each sensing period [18]. The trade-off for this improved resolution is additional overhead in communication between the wireless sensor network and the decision maker [18]. For a single channel *k*, the *n*-bit spectral scanning results comprise a two-dimensional matrix

$$\mathbf{M}^{(k)} = \left[m_{ij}^{(k)}\right]_{N\times N_P} \tag{40}$$

where

$$m_{ij}^{(k)} = \begin{cases} 0 & H_0 \\ 1,2,3,\ldots,2^n-1 & H_1 \end{cases} \tag{41}$$

is the *n*-bit spectrum sensing result for the *i*th sensor node in the *j*th spectral scan of channel *k*.

As in two-bit [22] and three-bit [18] hard combination, multiple energy detection thresholds are established to make the determination as to which energy region the received signal energy falls into [18], [22]. The thresholds are determined using Neyman-Pearson criterion [18], [22]. The $\overline{P_f}$ is fixed in advance while the $\overline{P_{d,i}^{(k)}}$ is maximized [18], [22]. The $\overline{P_f}$ values for each of the energy detection regions are shown in Table 1 [18]. The false alarm values for each threshold are determined by the coefficients β_n [18]. These coefficients are determined by [18]

$$\beta_n = 10^{-n}, \qquad n = 2,3,\ldots,2^n-1 \tag{42}$$

where n is the threshold index and $\beta_0 = 1$ [18]. As shown in [18], determining thresholds are design issues.

Table 1. Thresholds and false alarm values for n-bit spectrum sensing (From [18]).

Threshold	$\overline{P_f}$, False Alarm
λ_{2^n-1}	$\beta_{2^n-1}\overline{P_f}$
$\cdots$	$\cdots$
λ_3	$\beta_3\overline{P_f}$
λ_2	$\beta_2\overline{P_f}$
λ_1	$\beta_1\overline{P_f}$

Unlike two-bit hard combination, the presence of the user occupying the channel is not determined by the weighting scheme given by (3). Rather, the presence of the user occupying the channel is determined by the majority rule for binary spectrum sensing as previously discussed in Section B. To facilitate use of the majority decision rule, the n-bit spectrum sensing results are converted into binary spectrum sensing results in accordance with

$$x_{ij}^{(k)} = \begin{cases} 0, & m_{ij}^{(k)} = 0 \\ 1, & m_{ij}^{(k)} > 0 \end{cases} . \tag{43}$$

The binary spectrum sensing results are then used to filter the n-bit spectrum sensing results by

$$\begin{aligned} \tilde{\mathbf{M}}^{(k)} &= \mathbf{M}^{(k)}\mathbf{Y}_{\mathbf{M}}^{(k)} \\ &\triangleq \left[\tilde{m}_{ij}^{(k)}\right]_{N\times N_P} . \end{aligned} \tag{44}$$

Finally, a weighted estimate of $\overline{P_{d,i}^{(k)}}$ is obtained as

$$\overline{P_{d,i}^{(k)}} = \frac{\sum_{j=1}^{T_P} m_{ij}^{(k)}}{\operatorname{tr}\left(\mathbf{Y}_{\mathbf{M}}^{(k)}\right)\times 2^n} . \tag{45}$$

E. POSITION REFINEMENT IN THE ESRB LOCALIZATION SCHEME

The incorporation of position refinement in the ESRB localization scheme is shown in Figure 12. The position refinement process takes place at the decision maker. The purpose of the position refinement function is to manage the history of the potential secondary users discovered in the environment. This includes refining previous position estimates for users of interest already discovered. The position refinement function consists of two sub-functions: 1) spectrum sensing isolation and 2) secondary user position refinement.

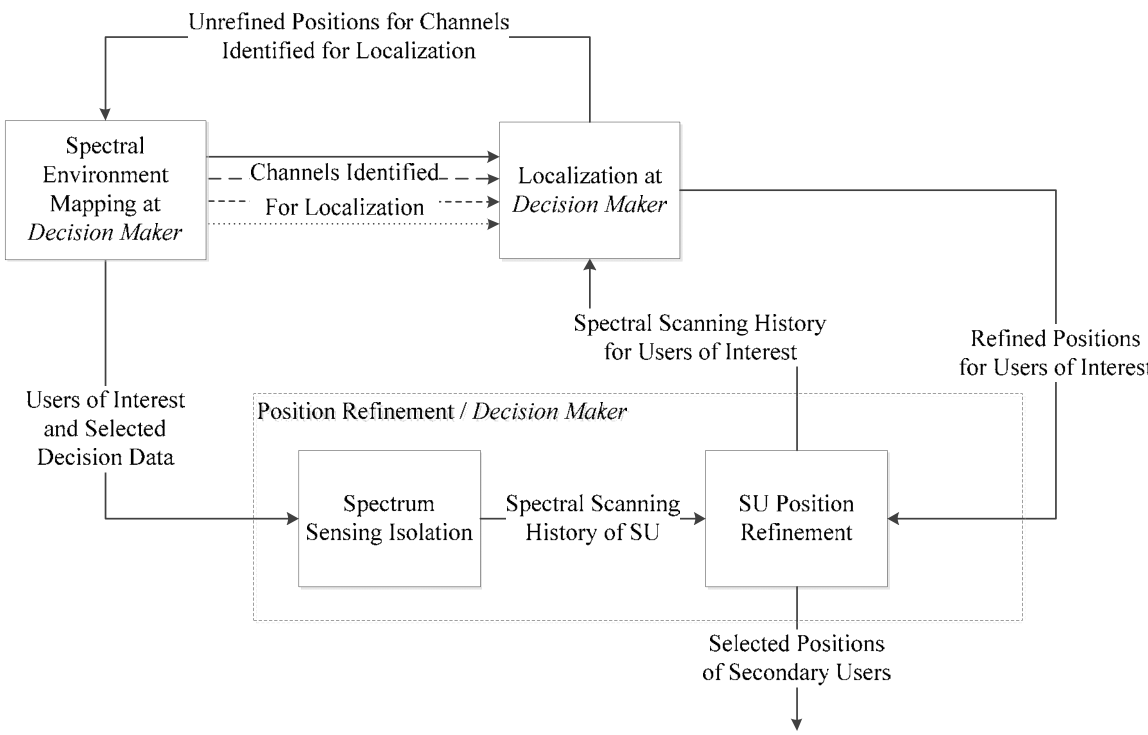

Figure 12. Detailed conceptual diagram of position refinement in the proposed ESRB localization scheme for cognitive radio positioning.

1. Using Position Estimation to Track Frequency

The essence of the position refinement function is managing the secondary user history at the decision maker. Through this process the decision maker is able to track the channel occupancy of secondary users based on estimates of their position. Users of interest and their selected decision data become available after N_P spectral scans from

the spectral environment mapping function. As time progresses, new users of interest will become identified after another N_P spectral scans have taken place. The position refinement process determines if the newly discovered users match the positions of any previously discovered users. If so, the matched users' channels and position estimates are recorded under the previously discovered users' information. In this way, as multiple secondary users move into new channels over time, the decision maker is able to track which channels have been occupied by the same user. This process begins with the spectrum sensing isolation sub-function.

2. Isolating Spectrum Sensing Results

The goal of the spectrum sensing isolation sub-function is to pair old spectrum sensing decision data to new decision data for matching position estimates. This is accomplished by determining if any new position estimates fall within a radius of tolerance from old position estimates for users of interest. If a match is found, then the old and new spectral scanning results from the wireless sensor network are merged. If a match is not found, then the newly discovered user is considered a different user and not considered to be one of the users previously recorded prior to that point in time. The unmatched user is recorded in the secondary user history without any relationship to any previously discovered results. The number of times a user has been successfully paired with new measurement results is also recorded for each user contained in memory. Those users, which have been discovered more than once, are declared to be secondary users.

3. Position Refinement

As decision data is aggregated by the spectrum sensing isolation sub-function, the secondary user position refinement sub-function reevaluates the position estimate of all potential secondary users. With additional spectral scans available for matched users of interest, the localization process is capable of increasing the accuracy of the position estimate. These position estimates are fed back into the position refinement process and recorded in memory. As additional decision data is made available through the spectrum

sensing isolation sub-function, the position refinement process is repeated to continue updating potential secondary users' positions.

An in-depth explanation of the proposed ESRB localization scheme was provided in this chapter. Four aspects of the scheme were examined in detail: 1) cooperative spectrum sensing, 2) spectral environment mapping, 3) localization through the iterative NLSM, and 4) position refinement. It was proposed that *n*-bit spectrum sensing may improve the performance of the iterative NLSM through accurate estimation of $\overline{P_{d,i}^{(k)}}$ in a shorter period of time than binary spectrum sensing. The performance of the proposed ESRB localization scheme is demonstrated through simulation in the following chapter. Specifically, an in depth examination of the simulation scenario, simulation model, and results are provided, which illustrate the strengths and weaknesses of the proposed ESRB localization scheme.

THIS PAGE INTENTIONALLY LEFT BLANK

IV. SIMULATION MODEL AND RESULTS

A detailed explanation of the ESRB localization scheme was provided in Chapter III. The proposed scheme was summarized by its four primary functions: 1) cooperative spectrum sensing, 2) spectral environment mapping, 3) localization through the iterative NLSM, and 4) position refinement. An implementation of the ESRB localization scheme in a specific simulation scenario and a simulation model is presented in this chapter to demonstrate its performance. The simulation scenario and simulation model are described in detail in the sections immediately following. Power estimation and the effects of *n*-bit spectrum sensing, the number of spectral scans, and the number and position range of sensor nodes on the ESRB localization scheme are shown in Section C. Frequency mobility, spatial mobility, and scalability of the proposed scheme are addressed in the instantaneous results shown in Section D.

A. SIMULATION SCENARIO

The overall simulation scenario was originally introduced in Figure 1. It is presented again, in greater detail, in Figure 13 to give a clearer picture of how the ESRB localization scheme is implemented. In this scenario, three networks are present: 1) the primary user network, 2) the secondary user network, and 3) the wireless RF sensor network. A frequency-division multiple access (FDMA) network is assumed for the primary user network. That is, the entire frequency spectrum is broken up into a series of non-overlapping frequency bands or channels [5]. All channels are assumed to have one primary user present. Each primary user operates in one channel of the entire frequency band at random discrete intervals, leaving unused portions of the frequency spectrum available over time. All secondary users attempt to transmit at each corresponding time interval as the primary users do; however, the secondary users may transmit only over unused portions of the frequency spectrum. In addition, only one secondary user is assumed able to transmit in one unoccupied channel in one time interval. If more than one unoccupied channel is available, then more than one secondary user can transmit.

Secondary users perform spectrum sensing to determine where white spaces exist to facilitate continual transmission without incumbent interference [1], [19].

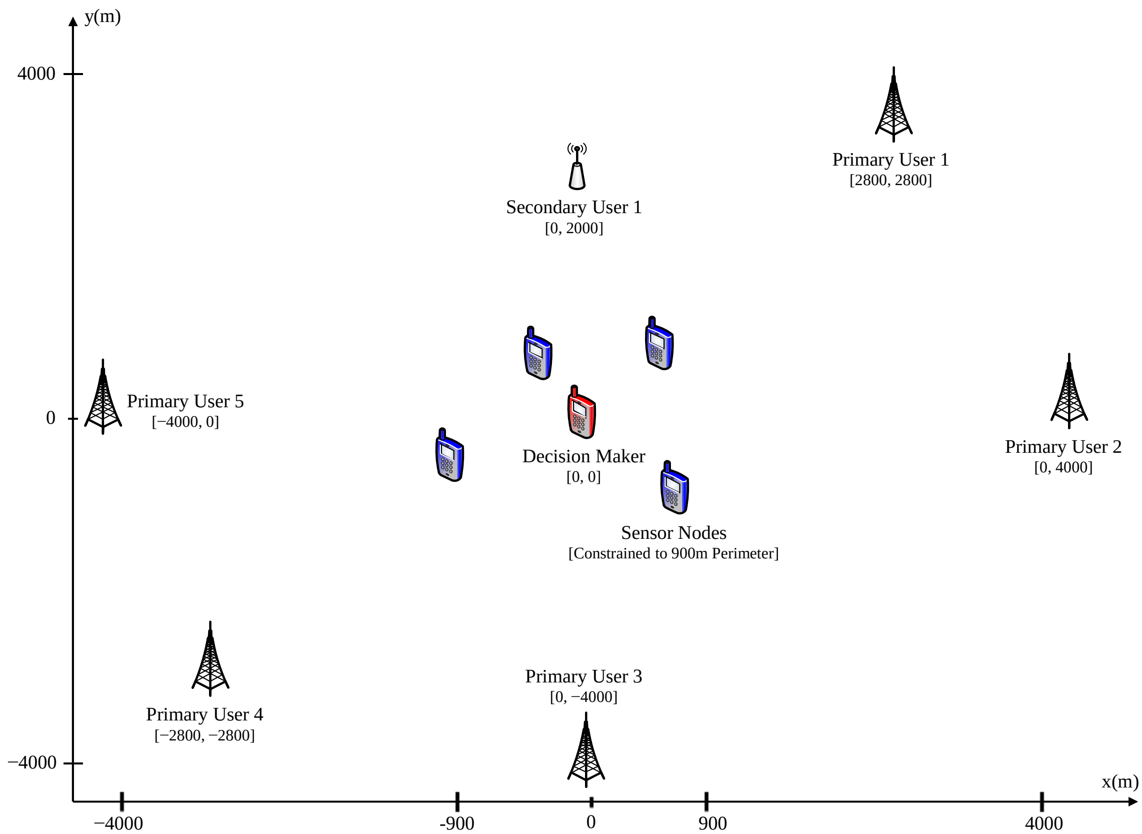

Figure 13. Simulation scenario using a wireless RF sensor network to determine the frequency bands and location of a stationary cognitive radio.

The wireless RF sensor nodes are randomly dispersed within a confined geographic area around the decision maker. All sensor nodes perform spectrum sensing in each channel across the entire frequency band of interest. Path loss, shadowing, multipath fading, and noise all influence the spectrum sensing results of the sensor nodes [5], [17]. However, the channel is assumed to be time-invariant during each spectrum sensing period [5], [17]. The sensor nodes are assumed to be capable of sensing the spectrum in a much shorter time interval than the occupancy duration of the primary or secondary users [1]. The decision maker, at the origin, collects the spectrum sensing results of the sensor network and estimates the position of all secondary users in the

environment using the ESRB localization scheme. The positions of the primary users and secondary users are assumed stationary during each localization process [5]; however, limited mobility is added to the secondary user for evaluating the instantaneous performance of the ESRB localization scheme in Section D. The positions of all sensor nodes are assumed to be known in advance by the decision maker [5], [17].

The random channel occupancy behavior of the primary user is driven by a discrete time two-state Markov model as shown in Figure 14. The primary user moves between an 'idle' or 'busy' state for various discrete lengths of time as determined by the probabilities p_i and p_b, respectively [5]. During the 'busy' state, the primary user continuously transmits a fixed amplitude signal. During the 'idle' state, no traffic is broadcast, leaving white space in the frequency spectrum [5], [17].

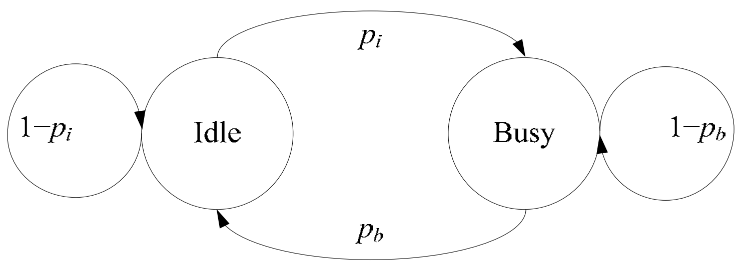

Figure 14. Two-state Markov model of primary user channel occupancy [5].

The basis for spectrum sensing behavior of all secondary users is the IEEE 802.22 standard [1], [19]. As discussed in Chapter II.C, the IEEE 802.22 standard dictates the use of quiet periods for spectrum sensing across the cognitive radio network [1], [19]. As such, QP are introduced into the data traffic of all secondary users in the simulation scenario. Specifically, fast and fine spectrum sensing periods are assigned with random uniform probabilities p_r and p_v within the superframes and MAC frames of the secondary user transmissions [1], [19]. The assumption is made that the secondary user will determine if a channel is occupied only after fast and fine spectrum sensing have taken place [1], [19]. Thus, the duration of one superframe is the most discrete unit of time a secondary user is assumed to be stationary in one channel of the frequency spectrum [19]. For purposes of the simulation scenario, it is also the most discrete unit of

time one primary user will occupy a channel. When white space has been identified and chosen by the secondary user, transmission consists of a fixed amplitude signal. No transmission occurs during designated quiet periods within superframes or MAC frames [1], [19].

The behavior of the wireless sensor network and the decision maker is in accordance with the ESRB localization scheme described in Chapter III. The sensor nodes conduct spectrum sensing in each channel across the entire frequency band of interest and report their spectrum sensing results to the decision maker as a single spectral scan. The assumption is made that no errors occur in transmission of decision data to the decision maker and that all decision data is transmitted instantaneously [5], [17]. In turn, the decision maker aggregates the spectral scanning results of the wireless sensor network and develops a global channel occupancy map. From the channel occupancy map, the decision maker identifies which channels are occupied and which are not over the time duration of the spectral scans received. For the purposes of the simulation scenario, this occurs after every superframe in the secondary user network. Shadowing, as a form of medium scale fading, is assumed to be deterministic during each superframe but varies between superframes as a random variable [5]. The decision maker localizes the users within the occupied channels to discriminate, which users are primary users and which are potential secondary users. Potential secondary users are labeled as users of interest, and their position estimates are stored in memory at the decision maker along with the sensor network's spectral scanning results for that channel. As additional spectral scans become available, the decision maker refines the position estimates for all users of interest stored in memory. If the position estimate of a user of interest is confirmed more than once, it is considered to be a secondary user.

B. SIMULATION MODEL

The exact simulation model of the simulation scenario previously described is shown in Figure 15. Five primary users and one secondary user are assigned stationary positions in accordance with the coordinates listed in Table 2. The primary users' busy and idle probabilities p_i and p_b, respectively, are both set to 0.3 to ensure enough white

spaces exist for the secondary user to always have a channel available for transmission. The transmission powers of the primary and secondary users are set to 18 Watts and 16 Watts, respectively. These transmission powers are set close to one another to remove power as a distinguishing feature between primary and secondary users, although in practice the transmission power of the secondary user may be much less than the primary user [1], [19].

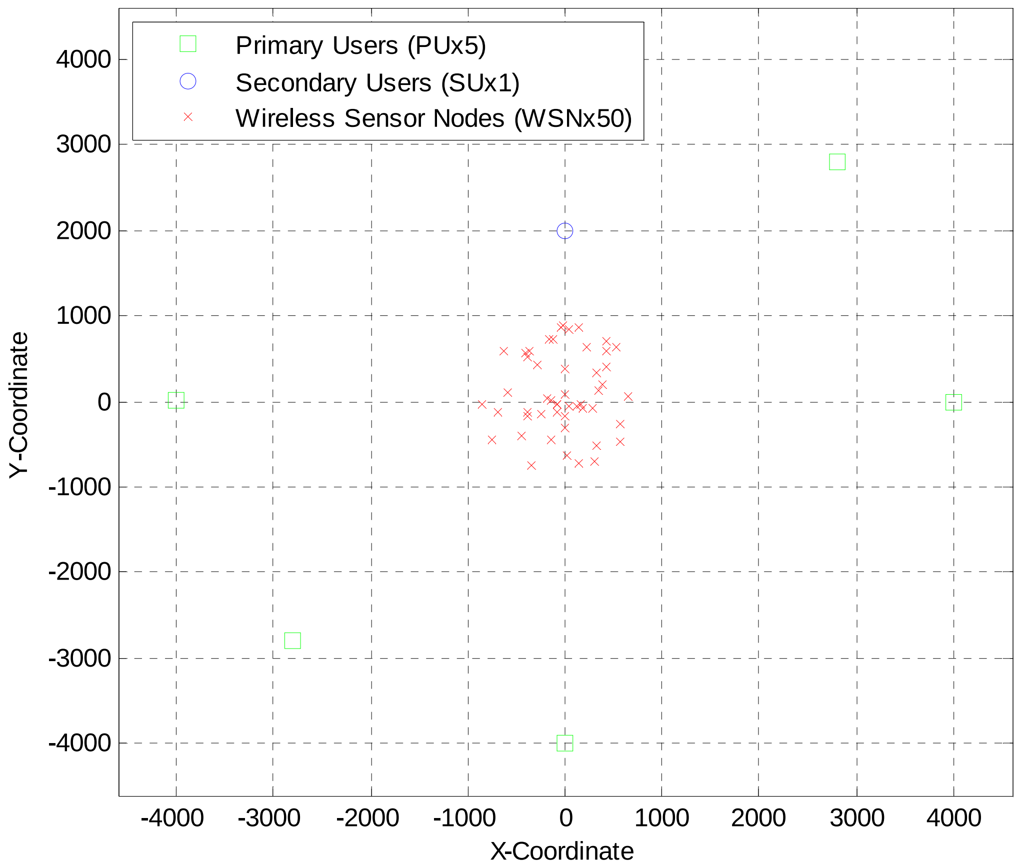

Figure 15. Simulation model using a wireless RF sensor network to determine the frequency bands and location of a stationary cognitive radio.

Table 2. Primary and secondary user coordinates used to study the effects of various parameters on the ESRB localization scheme.

Users	X-Coordinates (m)	Y-Coordinates (m)
Primary User 1	2800	2800
Primary User 2	0	4000
Primary User 3	0	-4000
Primary User 4	-2800	-2800
Primary User 5	-4000	0
Secondary User 1	0	2000

The secondary user's fast and fine sense probabilities p_r and p_v, respectively, are set to 0.65 and 0.45, respectively. A probability greater than 0.5 was assumed for fast sensing to ensure on average spectrum sensing took place within the majority of MAC frames [1], [19]. Fine spectrum sensing is assumed to take place less often as the secondary user network desires to maintain a high quality of service (QOS) and, therefore, only engages in fine sensing when necessary. Hence, the probability p_v is set much lower than p_r [1], [19].

Fifty sensors nodes are uniformly distributed at random within a 900 meter perimeter from the decision maker at the origin. No sensor node is allowed within 50 meters of the decision maker's position to ensure adequate spatial separation during spectrum sensing. The positions of all sensor nodes are randomly assigned each simulation run. The $\overline{P_f}$ is set to 0.01 for all sensor nodes. Using (10) and defining a time-bandwidth product u of 5.0, we derived an energy detection threshold λ of 13.96 for all sensor nodes.

The following channel conditions are defined to facilitate path loss, shadowing, multipath fading, and noise in the simulation model. Path loss and noise are modeled using (8) where the constant c is set to 0.01, the path loss exponent α is set to 3, and noise variance σ_0^2 is set to –90 dBm [17]. Shadowing is modeled as a log-normal distribution and is defined as [5], [18]

$$S = 10^{\frac{\vartheta_s}{10}} \tag{46}$$

where ϑ_S is a Gaussian random variable with a mean of zero and standard deviation σ_s of one. To implement the effects of shadowing in the simulation model, (8) is modified as

$$\overline{\gamma_i^{(k)}} = \frac{cP_{tx}^{(k)}\left(d_i^{(k)}\right)^{-\alpha} S}{\sigma_0^2} \quad (47)$$

As discussed previously in the simulation scenario, the random variable ϑ_s is constant throughout each superframe but is randomly changed between superframes in accordance with (46). Multipath fading is modeled using (9) where $\overline{\gamma_i^{(k)}}$ is modeled using (47).

The initial power estimate $\hat{P}_{tx}^{(k,0)}$ at the decision maker is set to 17 Watts, the median transmission power of the primary and secondary users. The radius of tolerance for accepting an unrefined position estimate as a primary user or secondary user is set to 750 meters. During the localization process, ε (i.e., the level of tolerance in the difference between position estimates after each iteration of the iterative NLSM) is set to one. If the position estimate falls within the perimeter of the wireless sensor network, the decision maker assumes the localization attempt has diverged and ignores the position estimate.

To study the effects of various parameters on the performance of the ESRB localization scheme, the simulation model is run approximately 1000 times. Unless otherwise indicated, each simulation execution is run for 10 superframes with the wireless sensor network performing 600 spectral scans per superframe. The root-mean-square error (RMSE) ξ_{RMSE} over all simulation executions is used as the performance metric to determine the effectiveness of the ESRB localization scheme. The RMSE ξ_{RMSE} is determined in accordance with

$$\xi_{RMSE}\left(\hat{d}_{error}\right) = \sqrt{E\left[\hat{d}_{error}^{\;2}\right]} \quad (48)$$

where $\hat{d}_{error}$ is the distance error of the position estimate of the secondary user after each simulation execution. The simulation is implemented in the MATLAB programming

language. The effects of varying multiple parameters on the ESRB localization scheme can be seen in the following sections.

C. ESRB LOCALIZATION RESULTS

1. Effects of *n*-bit Spectrum Sensing

The benefits of using *n*-bit spectrum sensing and (45) to obtain $\overline{P_{d,i}^{(k)}}$ are shown in Figure 16 and Figure 17. The divergence percentage of the iterative NLSM and ξ_{RMSE} of the secondary user position estimate are used as performance metrics to evaluate the efficacy of the proposed ESRB localization scheme. The divergence percentage is determined by

$$D_{\%} = \frac{\text{Number of Localization Attempts where Divergence Occurs}}{\text{Total Number of Localization Attempts}} \times 100 \,. \qquad (49)$$

The effects of the number of spectral scans on divergence percentage as a function of the number of bits in the *n*-bit spectrum sensing process are shown in Figure 16. The divergence percentage for binary (i.e., 1-bit) spectrum sensing declines exponentially as the number of spectral scans increases linearly. However, using two-bit and three-bit spectrum sensing, the divergence percentage declines at an accelerated rate relative to binary spectrum sensing. Such acceleration indicates with higher bit-order spectrum sensing the number of localization attempts with divergence decreases as the bit-order increases. As an example, for two-bit or three-bit spectrum sensing, the divergence percentage is near zero for 500 spectral scans compared to almost 40% for binary spectrum sensing.   For more than three-bits, however, the percentage divergence does not outperform binary spectrum sensing when more than 400 spectral scans are available. Further work is needed to examine the effects of using more than 3-bits in the spectrum sensing process.

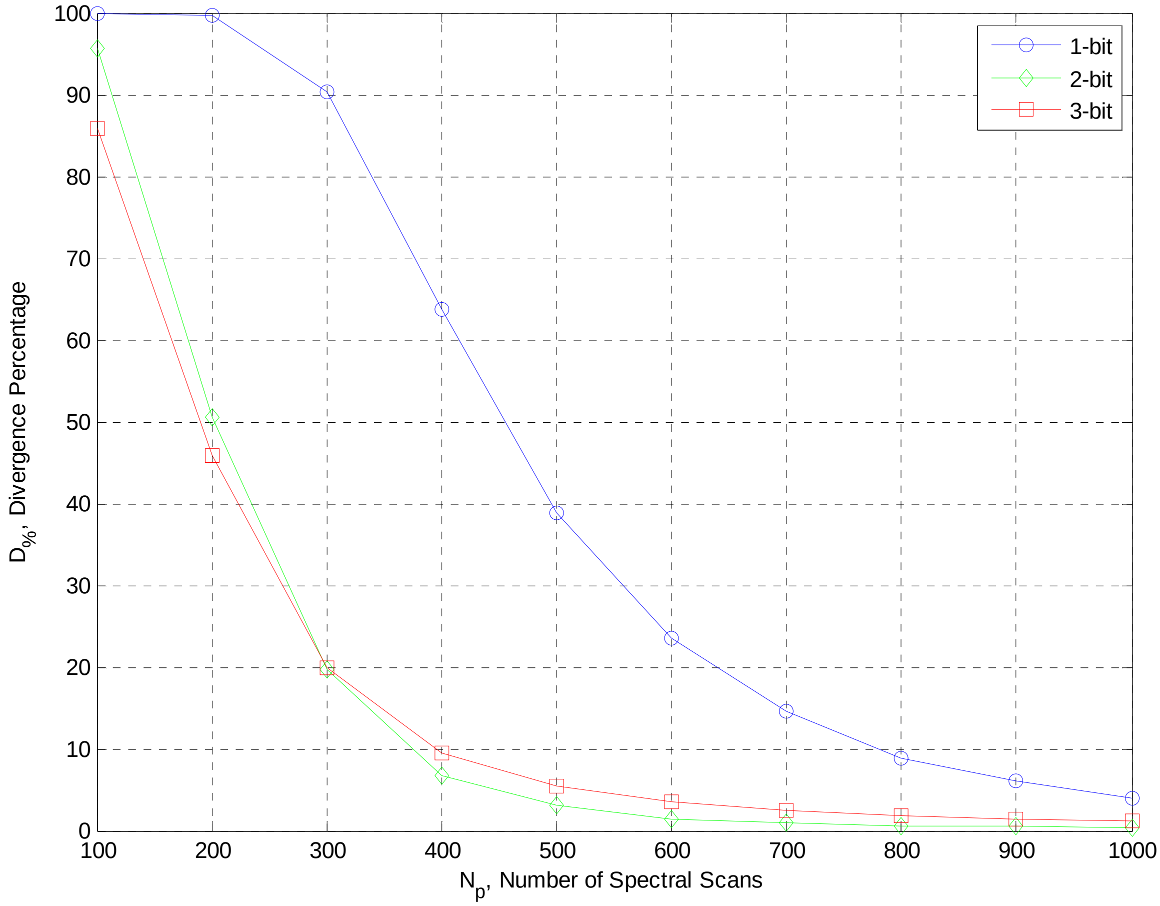

Figure 16. Divergence percentage versus the number of spectral scans for three different bits values in *n*-bit spectrum sensing.

The effects of the number of spectral scans on the RMSE of the position estimate as a function of the number of bits in the *n*-bit spectrum sensing process are shown in Figure 17. Under binary spectrum sensing, ξ_{RMSE} exponentially declines as the number of spectral scans increases linearly. However, in similar fashion to divergence percentage, both two-bit and three-bit spectrum sensing outperforms the use of a single bit in terms of position estimation. With the reduction in failed localization attempts from higher bit-order spectrum sensing, the ESRB localization scheme is able to develop a more accurate estimate of the secondary user's position using a reduced number of spectral scans. Furthermore, two-bit spectrum sensing outperforms three-bit spectrum sensing in terms of position estimation. Beyond 300 spectral scans, ξ_{RMSE} for two-bit spectrum sensing remains below three-bit spectrum sensing. Two-bit spectrum sensing is

capable of achieving significantly lower error performance while acheiving approximately the same decline in divergence percentage as three-bit spectrum sensing.

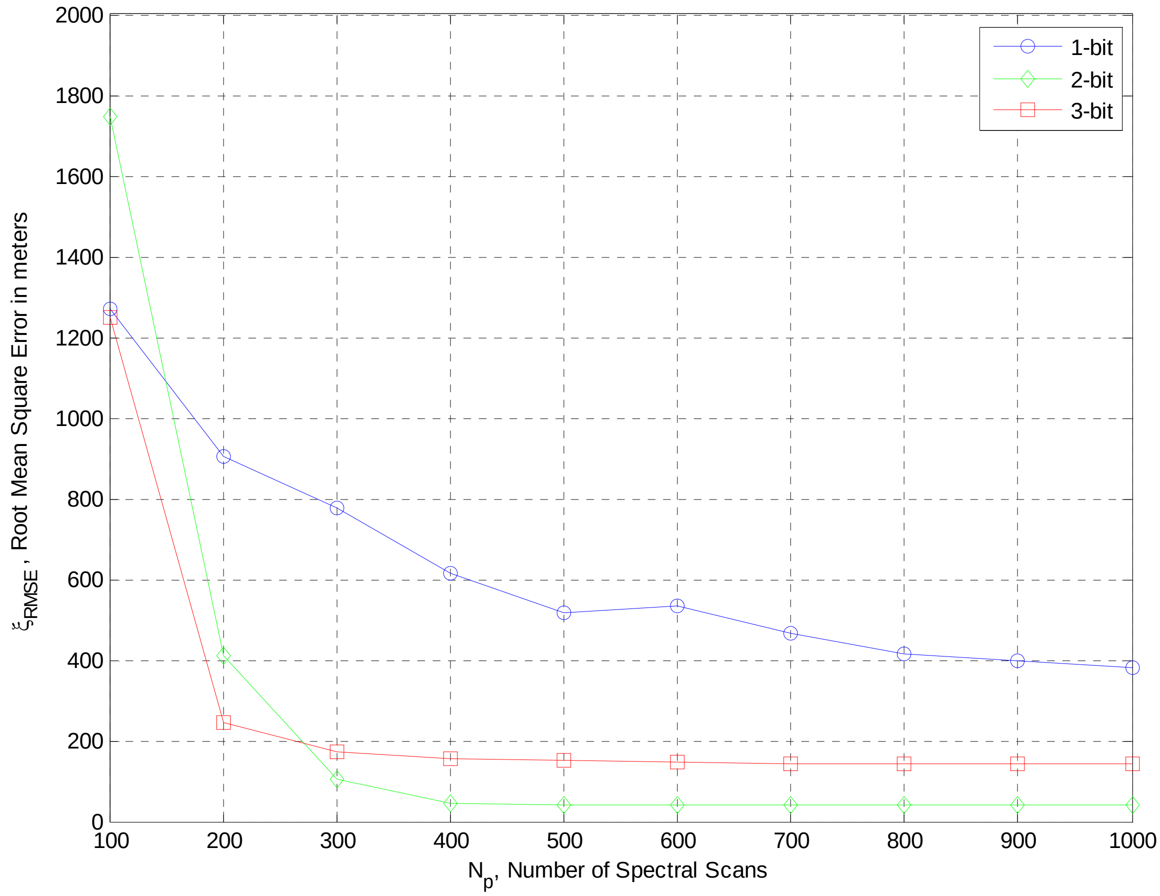

Figure 17. Position estimation RMSE versus the number of spectral scans for three different bit-level values in *n*-bit spectrum sensing.

In summary, the divergence percentage directly influences position estimation as each failed localization attempt reduces the ability of the ESRB localization scheme to accurately estimate the secondary user's position. This can be attributed to the weighting scheme of (45) on the estimates of $\overline{P_{d,i}^{(k)}}$. The measurement results of sensor nodes with extremely low probabilities of detection are suppressed as the number of bits in *n*-bit spectrum sensing increases. Measurement results of the sensor nodes with higher probabilities of detection are weighted more heavily. As a result, two-bit spectrum

sensing was used in all remaining simulations of the ESRB localization scheme due to improved performance in position estimation over three-bit spectrum sensing.

2. Effects of the Number of Spectral Scans per Superframe

The effects of the number of spectral scans per superframe on the RMSE of the position estimate of the secondary user as a function of the number of sensor nodes are shown in Figure 18. Two significant conclusions can be drawn from results shown in this figure. First, in general, regardless of the number of sensor nodes, as the number of spectral scans increases, the RMSE of the position estimate of the secondary user decreases. The reason for this behavior is that as the number of spectral scans increases a more accurate estimate of $\overline{P_{d,i}^{(k)}}$ is obtained. With a more accurate estimate of $\overline{P_{d,i}^{(k)}}$, a more accurate estimate of $\overline{\gamma_i^{(k)}}$ can also be obtained. Thus, the iterative NLSM is able to derive a more accurate position estimate of the secondary user overall.

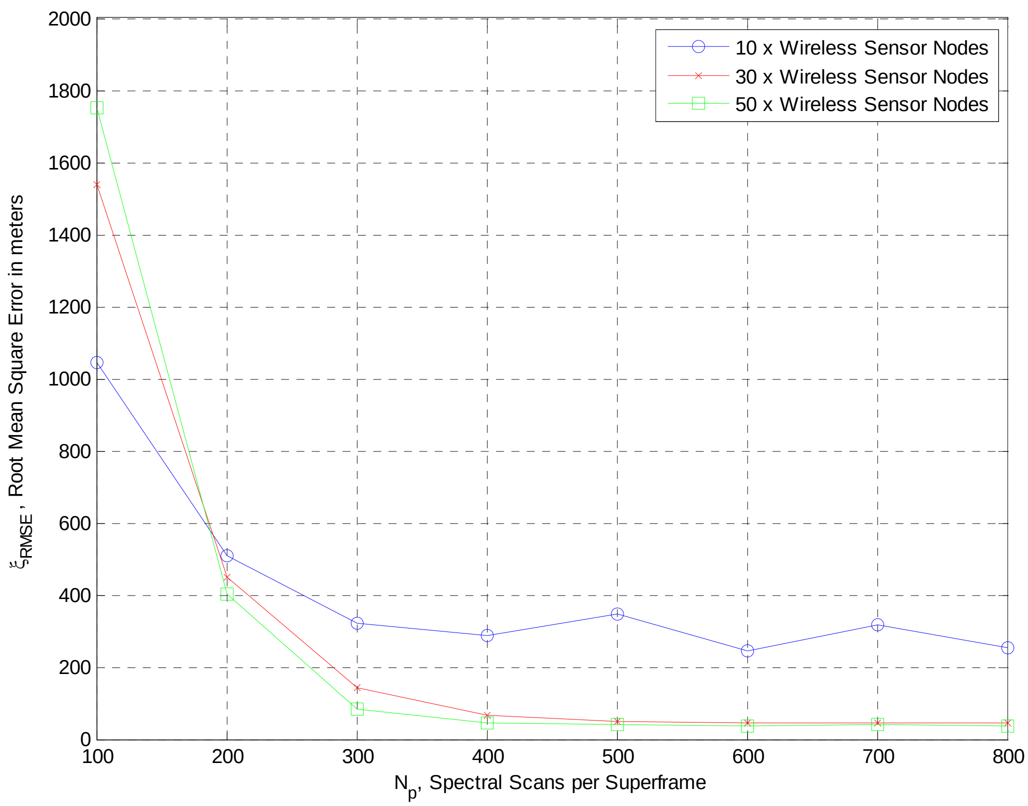

Figure 18. Position estimation RMSE versus the number of spectral scans per superframe for three different numbers of sensor nodes.

Second, as the number of sensor nodes increases, the RMSE of the position estimate of the secondary user decreases. This can be attributed to the collaborative spectrum sensing process and the iterative NLSM. Through collaborative spectrum sensing, as the number of sensor nodes increases a more accurate estimate of the global channel occupancy can be obtained by the decision maker. This in turn contributes to a more accurate estimate of $\overline{P_{d,i}^{(k)}}$, which, as stated previously, leads to a more accurate position estimate overall. Under the iterative NLSM as the number of nodes increases, more relevant decision data is available to derive the final position estimate. Thus, an initial estimate can be obtained closer to the true value. However, simply adding more nodes to the network is not sufficient. For additional decision data to be useful, adequate spatial separation must be maintained as will be shown in Section C.5.

3. Effects of the Number of Superframes

The effects of the number of superframes on the RMSE of the position estimate of the secondary user as a function of the number of spectral scans per superframe are shown in Figure 19. As illustrated by the figure, a more accurate estimate of the secondary user's position can be obtained as the number of superframes increases regardless of the number of spectral scans per superframe. This can be observed by comparing the rate of decline in ξ_{RMSE} when using 200, 400, or 600 spectral scans per superframe. When only 200 spectral scans per superframe are used, a significant drop occurs in ξ_{RMSE}. For 400 and 600 spectral scans, only a minor improvement in ξ_{RMSE} is observed relative to 200 spectral scans. Such benefit in ξ_{RMSE} with only 200 spectral scans can be attributed to the value of the position refinement process at the decision maker.

As previously shown in Section C.2, an increase in the number of spectral scans per superframe generates a more accurate estimate of the individual $\overline{P_{d,i}^{(k)}}$ leading to a more accurate overall position estimate. The same effect can be achieved by increasing the number of superframes over which the decision maker attempts to localize the secondary user. The spectrum sensing isolation sub-function takes each additional

superframe's relevant decision data and appends it to the appropriate user of interest in the decision maker's history. The position refinement sub-function then recalculates the position of all users of interest in memory with the new decision data. Thus, over time the decision maker can build up the necessary number of spectral scans to obtain an accurate position estimate rather than require the sensor network to achieve a large number of spectral scans each superframe. This benefit is substantial when considering the communication burden that must occur between the decision maker and the sensor network.

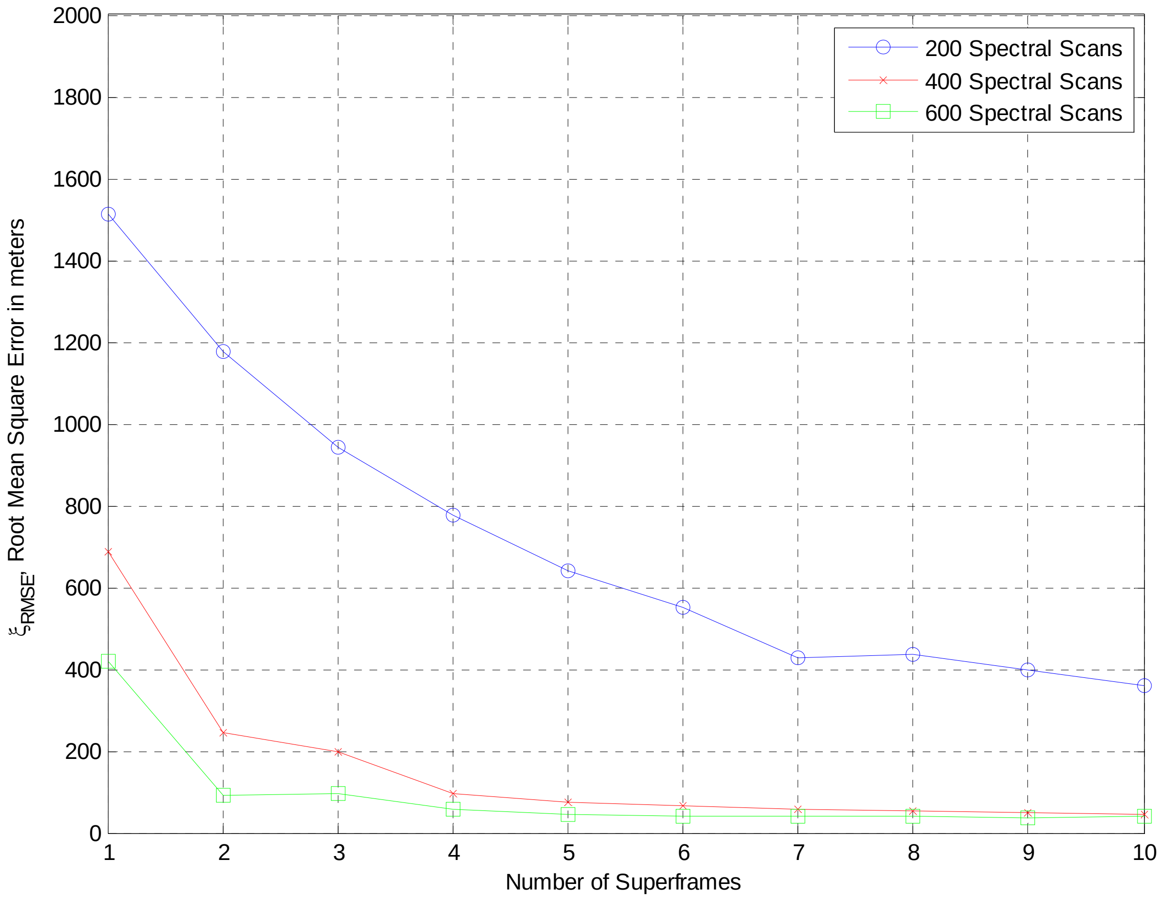

Figure 19. Position estimation RMSE versus the number of superframes for three different numbers of spectral scans per superframe.

4. Effects of the Number and Position Range of Wireless Sensor Nodes

The effects of the number of sensor nodes on the RMSE of the position estimate of the secondary user as a function of the number of spectral scans per superframe are

shown in Figure 20. The effects of the position range of the wireless sensor network on the RMSE of the position estimate of the secondary user as a function of the number of sensor nodes are shown in Figure 21. Of primary importance, the results depicted in both these figures indicates that the number of sensor nodes is not a significant factor, but rather spatial-sensing separation is the key characteristic which must be preserved for accurate position estimation [2]. The need for spatial-sensing separation is further confirmed in the relatively constant error in position estimation shown in Figure 20 regardless of the number of wireless sensor nodes. This constant error contrasts heavily with the significant decrease in accuracy shown in Figure 21 when the sensor network is restricted to a small perimeter. Such decline in accuracy occurs regardless of the number of sensor nodes used, again illustrating the significance of spatial-sensing separation in the ESRB localization scheme.

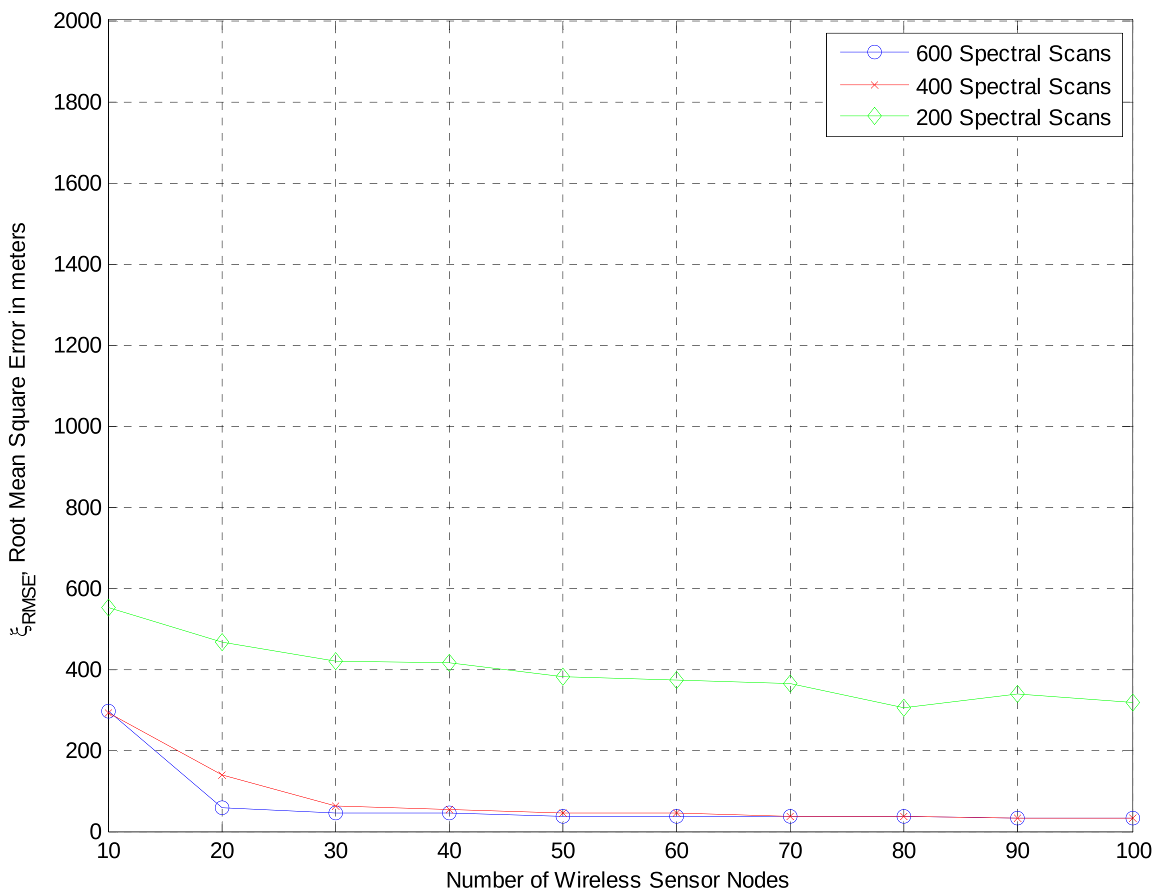

Figure 20. Position estimation RMSE versus the number of wireless sensor nodes for three different numbers of spectral scans per superframe.

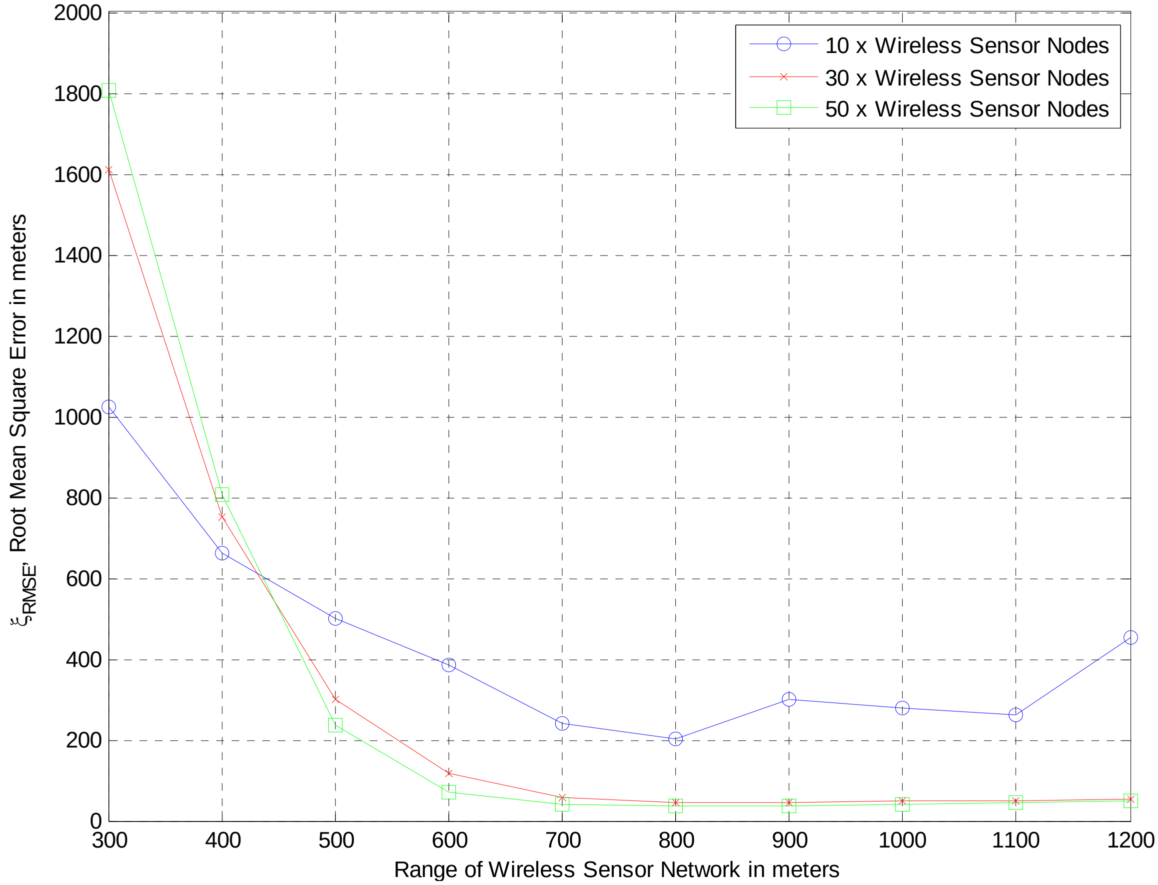

Figure 21. Position estimation RMSE versus the position range of wireless sensor network (WSN) in meters for three different numbers of sensor nodes.

5. Power Estimation

For all of the simulations conducted in the previous sections, the power of the primary users and the secondary user were assumed to be nearly the same to remove power as a distinguishing feature between the two different types of users. However, in practice, the secondary user is assumed to be using significantly less power than the primary user [1], [19]. For this reason, and to demonstrate the efficacy of the ESRB localization scheme in power estimation, the transmission power of the PU is set to 18 Watts and the transmission power of the SU is set to 4 Watts in this section. The initial power estimate $\hat{P}_{tx}^{(k,0)}$ at the decision maker is set to 11 Watts, the median transmission power of the primary and secondary users. The error in power estimation of the secondary user is shown in Figure 22. Similar to the results obtained in Section C.3, the

accuracy of the power estimation improves as the number of superframes increases. The reasons for the accuracy of the power estimate are the same reasons as position accuracy improvement as mentioned previously in Section C.3. The selective aggregation of relevant decision data over time allows the decision maker to improve the overall position and power estimate regardless of the fidelity in decision data obtained from each superframe.

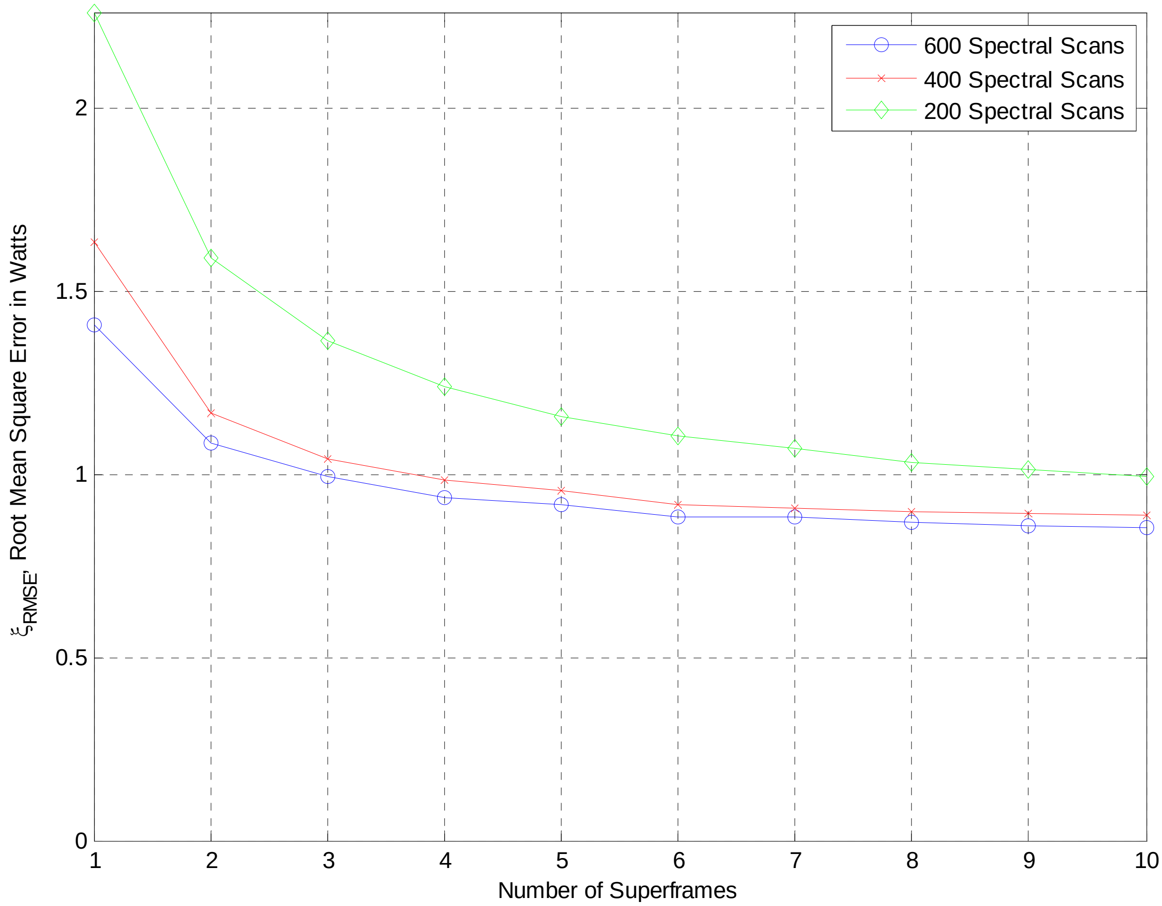

Figure 22. Power estimation RMSE versus the number of superframes for three different numbers of spectral scans per superframe.

D. INSTANTANEOUS ESRB LOCALIZATION RESULTS

The preceding simulation results were averaged outcomes of a large number of simulation executions. The following section presents instantaneous results of the ESRB localization scheme where the simulation model is run one to ten times under various conditions to determine its performance. The goal of this section is to illustrate the

impact of both frequency and spatial mobility of the secondary user on the ESRB localization scheme. The scalability of the ESRB localization scheme is also addressed.

1. Frequency and Spatial Mobility

The simulation scenario and simulation model are modified slightly to implement frequency and spatial mobility for the secondary user. These modifications are shown in Figure 23 and Figure 24, respectively. The single stationary secondary user shown in Figure 13 is replaced with a mobile secondary user in Figure 23 as indicated by the icon and its position change. The mobile user is assigned a single trajectory beginning at the same position as the stationary secondary user shown in Figure 13 and ending adjacent to the sensor network. All variables within the simulation environment are held the same as previously outlined in Section B except for the following assumptions. First, due to the mobile nature of the secondary user, the transmission power of the mobile cognitive radio device is assumed to be much less than the primary user network. As such, the secondary user's transmission power is set to 4 Watts, while the primary user transmission power remains at 18 Watts. The initial power estimate $\hat{P}_{tx}^{(k,0)}$ at the decision maker is set to 11 Watts, the median of the primary and secondary user's power.

Second, to facilitate motion, the mobile secondary user's speed is assumed constant throughout its movement along the predetermined trajectory. However, the position of the mobile secondary user is assumed constant during each localization attempt under the ESRB localization scheme. Specifically, the mobile secondary user is assumed to be in the same relative position throughout the duration of one superframe. As such, the decision maker is allowed only one superframe's worth of decision data from the sensor network to find the position of the mobile user. The ESRB localization scheme is attempted ten times during the movement of the mobile secondary user along its trajectory. The positions of the users in the environment are given in Table 3.

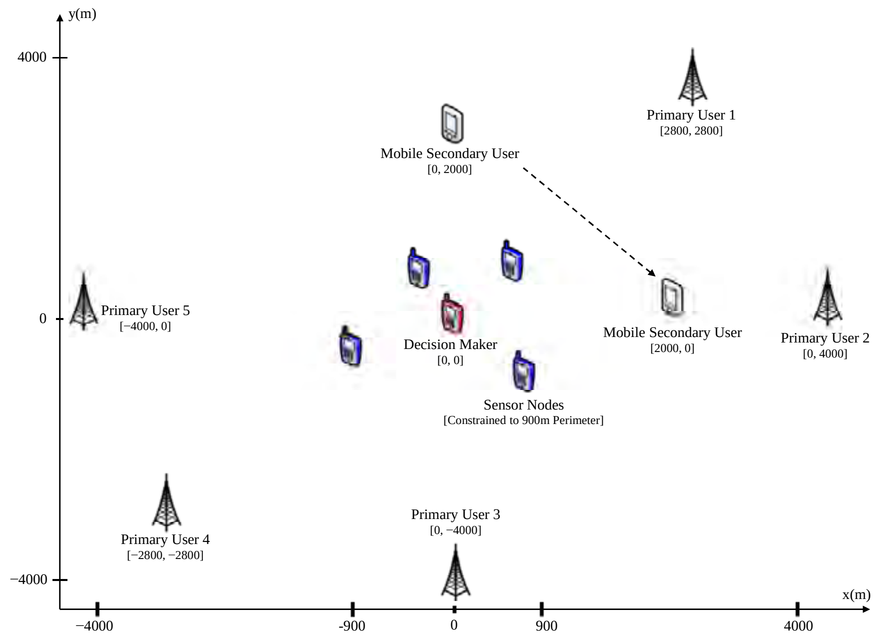

Figure 23. Simulation scenario using a wireless RF sensor network to determine the frequency bands and location of a mobile cognitive radio.

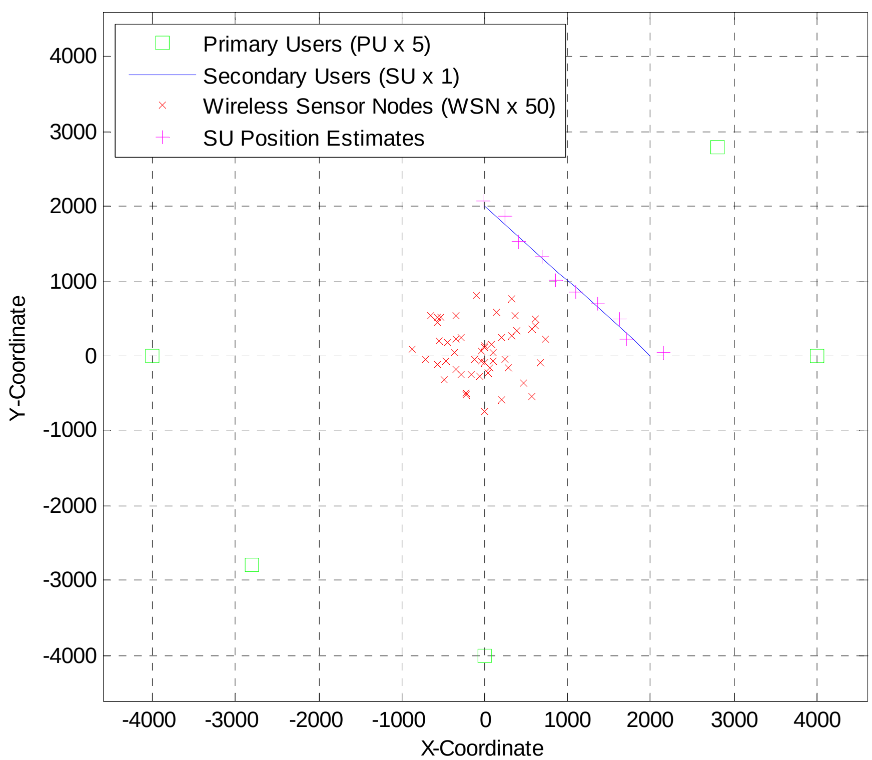

Figure 24. Simulation model and simulation results using a wireless RF sensor network to determine the frequency bands and location of a mobile cognitive radio.

Table 3. Primary and secondary user coordinates used to study the effects of a mobile secondary user on the ESRB localization scheme.

Users	X-Coordinates (m)	Y-Coordinates (m)
Primary User 1	2800	2800
Primary User 2	0	4000
Primary User 3	0	-4000
Primary User 4	-2800	-2800
Primary User 5	-4000	0
Secondary User 1 (Start Point)	0	2000
Secondary User 1 (End Point)	2000	0

The effects of frequency and spatial mobility of the mobile secondary user on the distance error of the position estimate of the mobile secondary user are shown in Figure 25 (a) and Figure 25 (b), respectively. Two important items can be gleaned from the results depicted in these figures. First, despite the position of the cognitive radio changing over time, the ESRB localization scheme is able to produce accurate position estimates evidenced by the low distance error during each ESRB localization attempt shown in Figure 25 (a). These same results are also represented in the spatial domain in Figure 24 where each secondary user position estimate is plotted. The reduced distance errors demonstrate the ability to perform limited tracking in the spatial domain using the proposed scheme. Second, the ESRB localization scheme is able to track the frequency band of operation of the mobile secondary user as it changes over time. This can be seen in the channel occupancy track of the decision maker displayed in the bottom of Figure 25 (b). During each localization attempt, the decision maker is able to find the channel of the secondary user as it moves to different portions of the frequency band of interest. Together, these results indicate source localization of a mobile cognitive radio is possible despite the shifting spatial, frequency, and temporal parameters. However, many of the assumptions made in the simulation scenario and simulation model may not always be valid. Further work is needed to improve the effectiveness of the ESRB localization scheme in tracking a mobile cognitive radio.

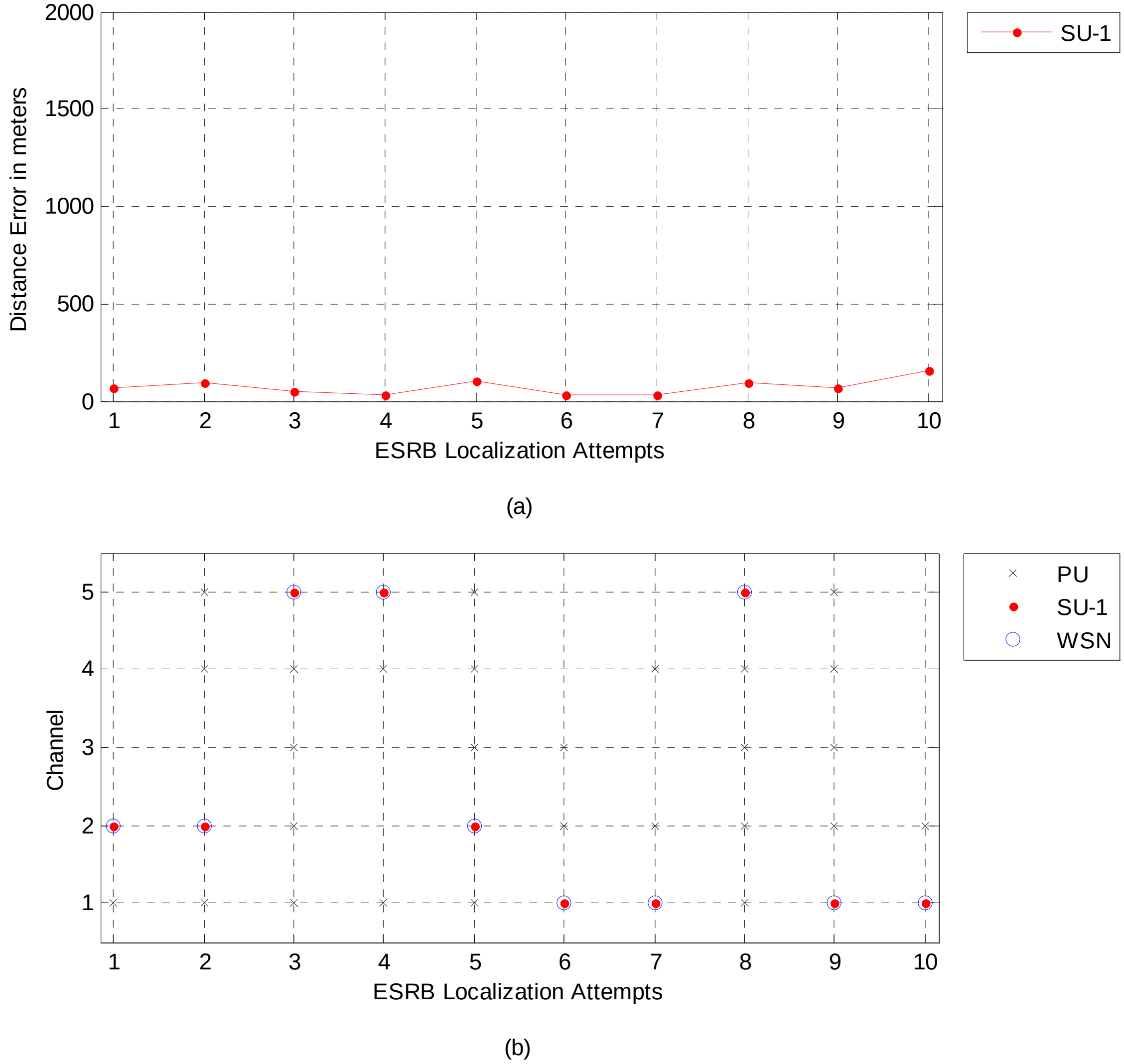

Figure 25. Secondary user frequency mobility and spatial mobility: (a) distance error versus the number of ESRB localization attempts to determine the location of a mobile cognitive radio, (b) channel occupancy versus the number of ESRB localization attempts to determine the frequency bands of a mobile cognitive radio.

2. Scalability of the ESRB Localization Scheme

The simulation scenario and simulation model are modified once again to address the scalability of the ESRB localization scheme. Multiple secondary users are placed in the environment to show whether or not the proposed scheme is capable of estimating the position of more than one secondary user. To implement this modification, the simulation scenario and simulation model is adapted to the environment depicted in

Figure 26 and Figure 27, respectively. Three stationary secondary users are placed at various positions in accordance with the user coordinates listed in Table 4. All variables within the environment are set to the values previously described in Section B except all three secondary user's transmission powers are set to 16 Watts. The simulation is run once over 15 superframes with 600 spectral scans per superframe by the sensor network. The ability of the ESRB localization scheme to determine the positions of multiple stationary cognitive radios is shown in Figure 28. The distance error for all three secondary users versus the number of superframes is shown in Figure 28 (a), and the channel occupancy versus the number of superframes is shown in Figure 28 (b).

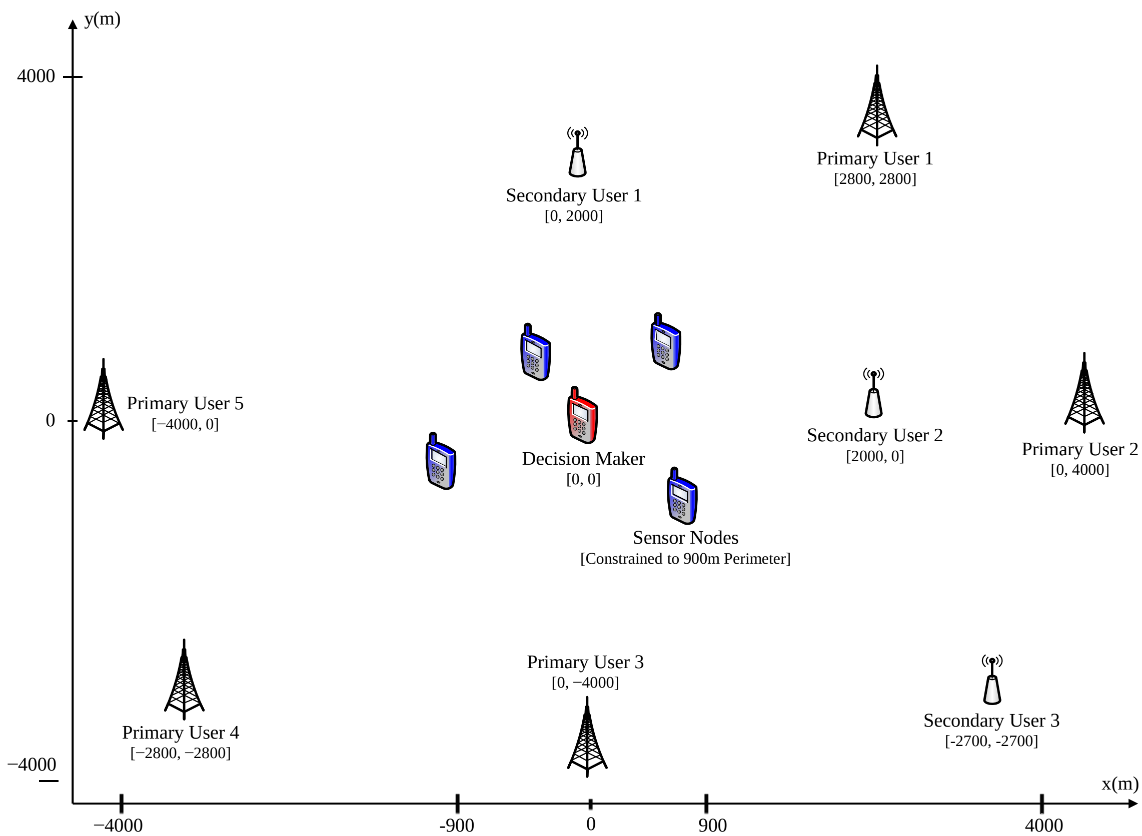

Figure 26. Simulation scenario using a wireless RF sensor network to determine the frequency bands and location of multiple stationary cognitive radios.

As previously shown in Section C.3, when the number of superframes increases the proposed scheme is capable of developing a more accurate estimate of the secondary

user's position. This same result is replicated for all three secondary users as evidenced by the decrease in distance error as the number of superframes increases. The increase in accuracy is directly tied to the ability of the decision maker to track each secondary user in the frequency domain. If the decision maker is not able to establish a correlation between the secondary user and the decision data received from the sensor network, then no position estimate can be achieved as illustrated by Secondary User 3. During the first superframe where no sensor network track is established, a position estimate is not achieved because not enough history is available for that particular secondary user. However, once Secondary User 3 is discovered in the second superframe, an accurate position estimate is achieved.

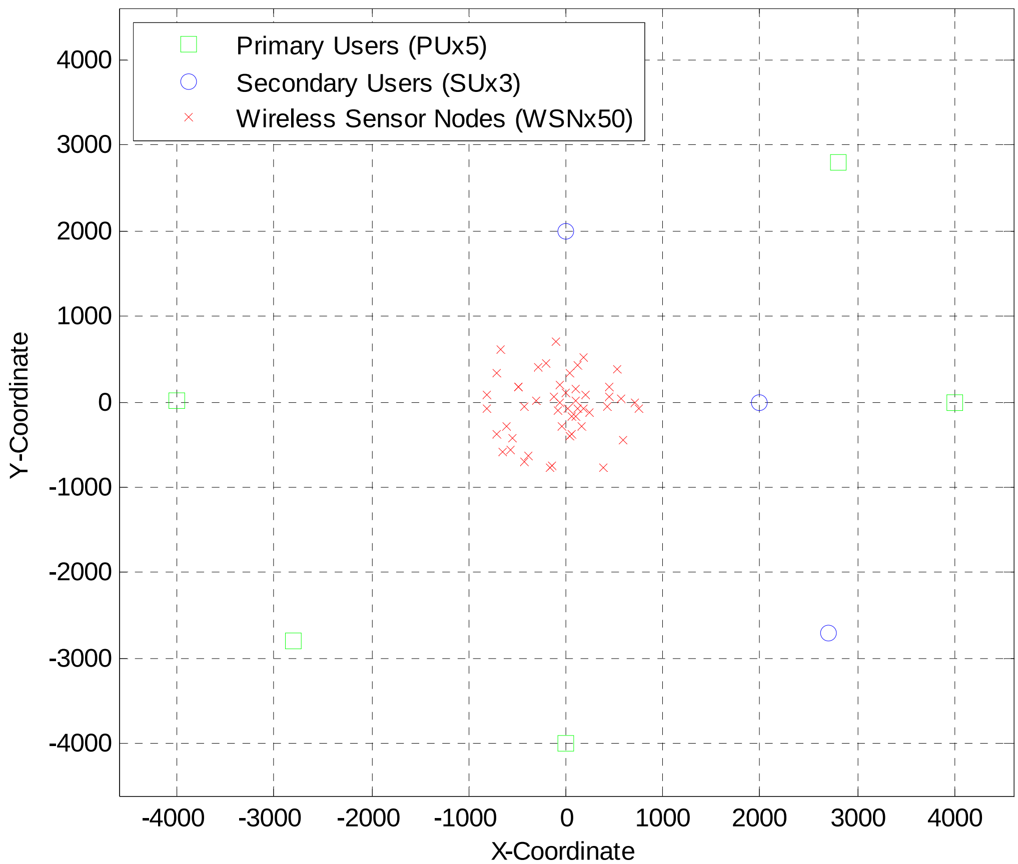

Figure 27. Simulation model using a wireless RF sensor network to determine the frequency bands and locations of multiple stationary cognitive radios.

Table 4. Primary and secondary user coordinates used to study the effects of multiple stationary secondary users on the ESRB localization scheme.

Users	X-Coordinates (m)	Y-Coordinates (m)
Primary User 1	2800	2800
Primary User 2	0	4000
Primary User 3	0	-4000
Primary User 4	-2800	-2800
Primary User 5	-4000	0
Secondary User 1	0	2000
Secondary User 2	2000	0
Secondary User 3	-2700	-2700

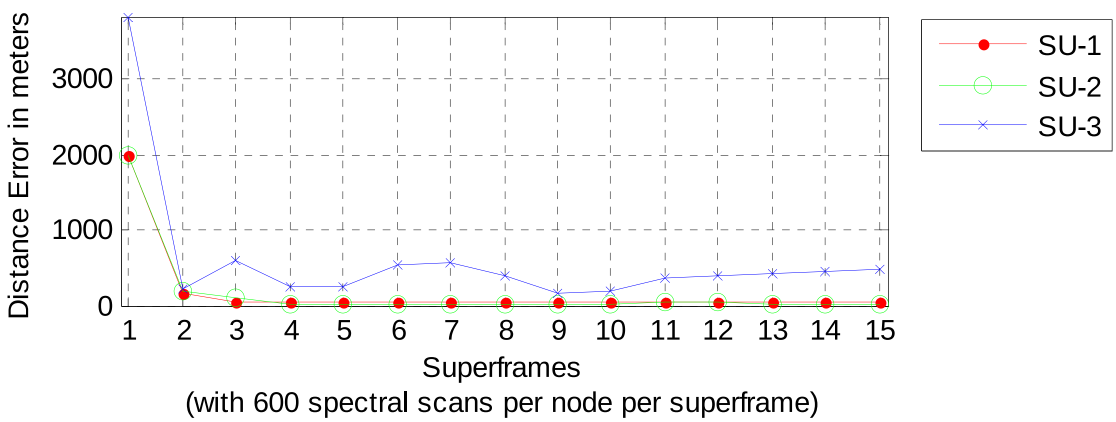

(a)

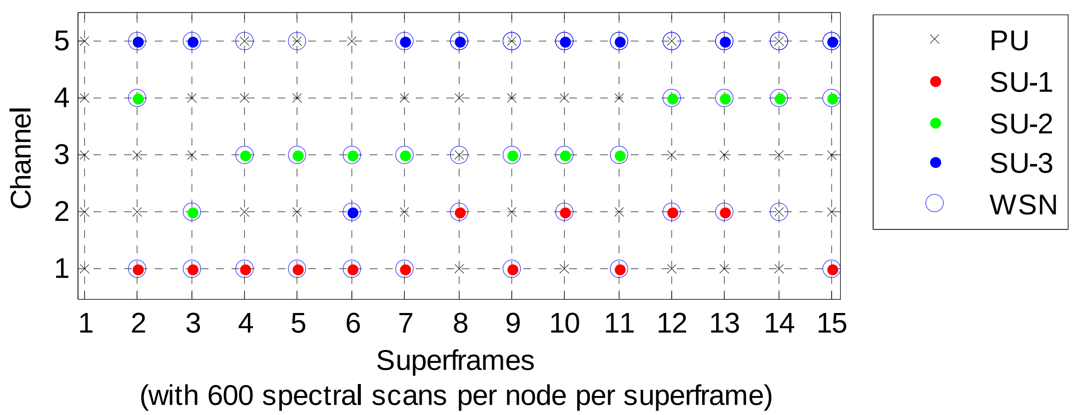

(b)

Figure 28. Multiple stationary secondary user localization: (a) distance error versus the number of superframes to determine the locations of multiple stationary cognitive radios, (b) channel occupancy versus the number of superframes to determine the frequency bands of multiple stationary cognitive radios.

The preceding simulation results indicate the ESRB localization scheme can be scaled to estimate the position of multiple stationary secondary users. However, the complexities involved with frequency and spatial mobility may hinder the scalability of the ESRB localization scheme in the context of mobile secondary users. Therefore, to completely address the scalability of the proposed scheme, the simulation scenario and simulation model are modified one final time to include multiple mobile and stationary secondary users. These modifications are shown in Figures 29 and 30, respectively.

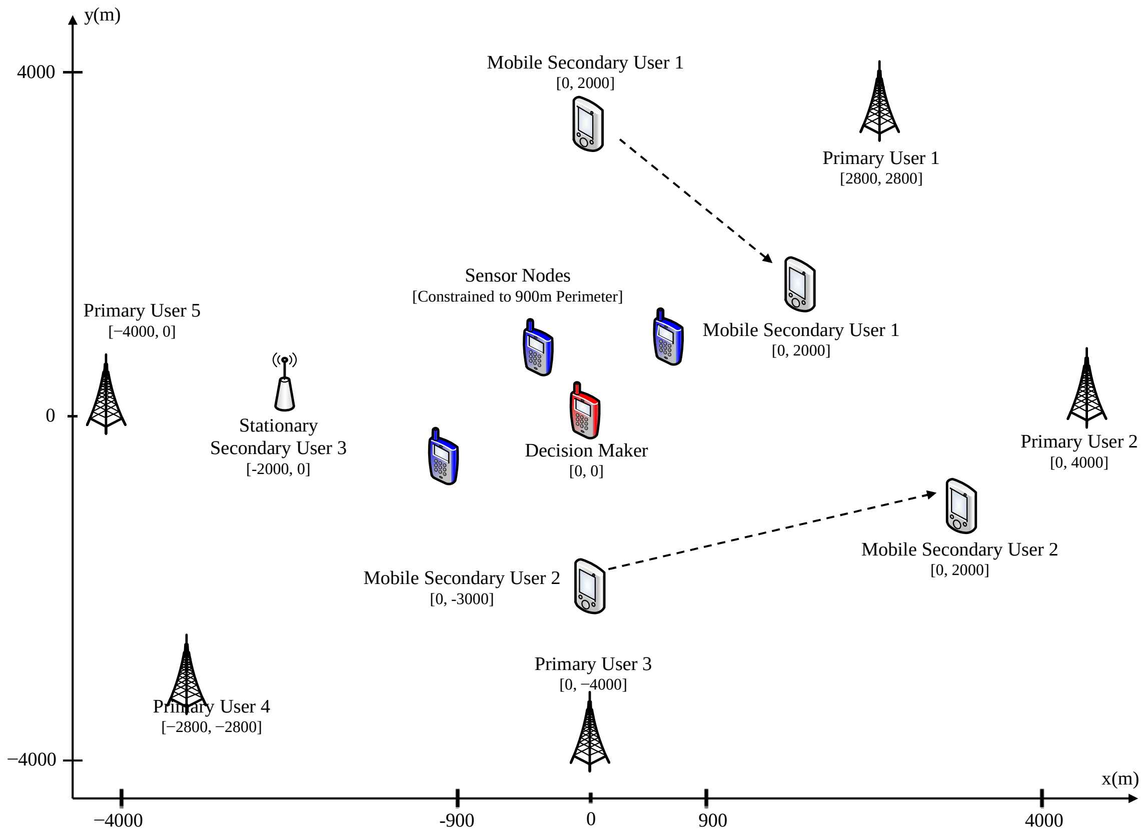

Figure 29. Simulation scenario using a wireless RF sensor network to determine the frequency bands and location of multiple mobile and stationary cognitive radios.

In the modified simulation scenario shown in Figure 29, three secondary users are present in the environment. Secondary User 1 and 2 are mobile and move along separate non-overlapping trajectories as indicated by the dashed lines in Figure 29 and the solid lines in Figure 30. Secondary User 3 is stationary in accordance with the user coordinates listed in Table 5. All variables within the environment are set to the values

previously outlined in Section B, except the transmission power for all three secondary users is set to 4 Watts. The same assumptions are made for each of the mobile secondary users as previously stated in Section D.1. The ESRB localization scheme is attempted ten times during the movement of all secondary users along their trajectories or fixed positions.

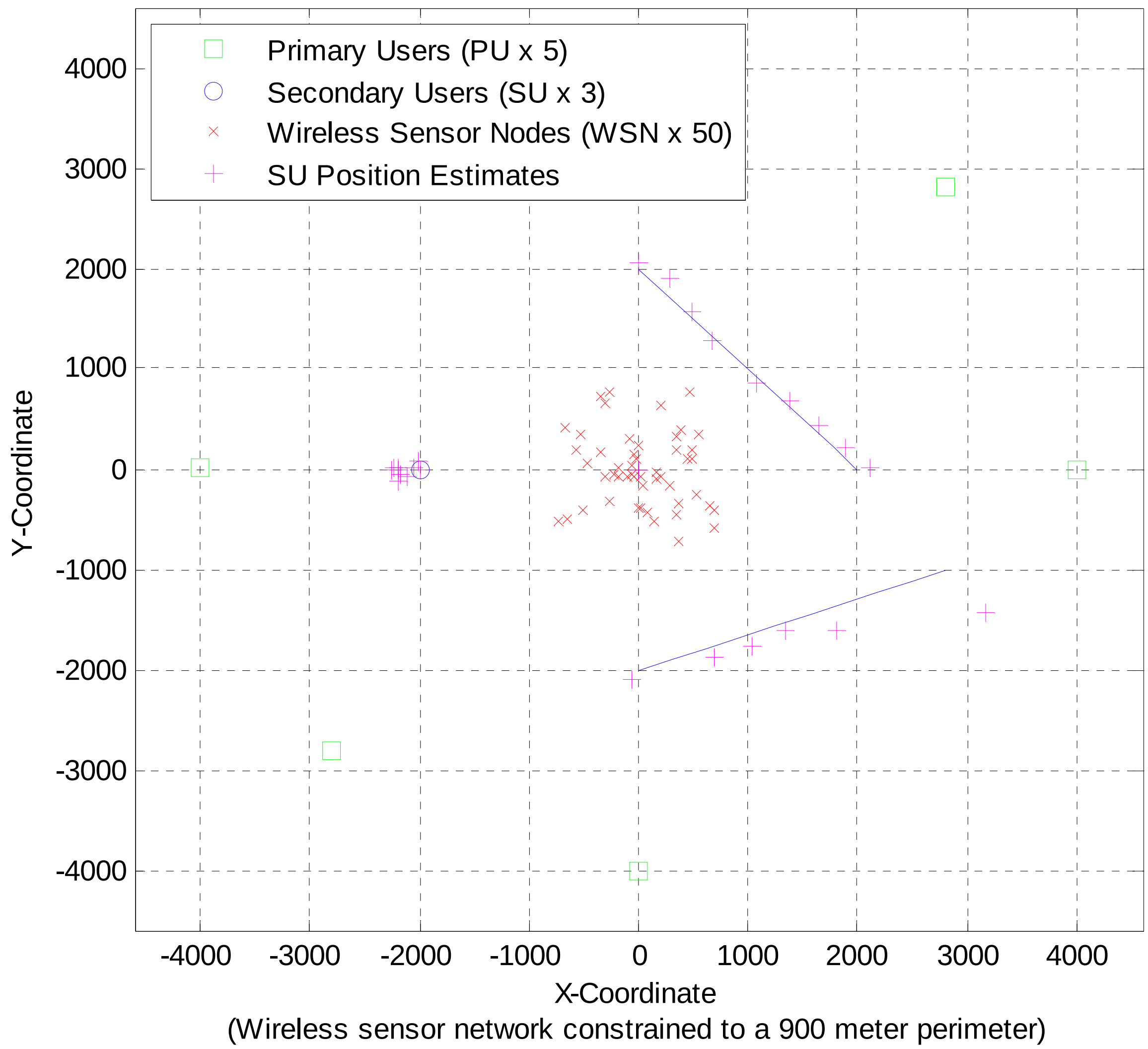

Figure 30. Simulation model and simulation results using a wireless RF sensor network to determine the frequency bands and location of multiple mobile and stationary cognitive radios.

Table 5. Primary and secondary user coordinates used to study the effects of multiple mobile and stationary secondary users on the ESRB localization scheme.

Users	X-Coordinates (m)	Y-Coordinates (m)
Primary User 1	2800	2800
Primary User 2	0	4000
Primary User 3	0	-4000
Primary User 4	-2800	-2800
Primary User 5	-4000	0
Secondary User 1 (Start Point)	0	2000
Secondary User 1 (End Point)	2000	0
Secondary User 2 (Start Point)	0	-2000
Secondary User 2 (End Point)	2800	-1000
Secondary User 3	-2000	0

The ability of the ESRB localization scheme to determine the positions of multiple mobile and stationary secondary users is shown in Figure 31. The distance error for all three secondary users versus the number of ESRB localization attempts is shown in Figure 31 (a) and the channel occupancy versus the number of ESRB localization attempts is shown in Figure 31 (b). Similar to the results obtained in Section D.1, the proposed scheme is able to perform limited tracking in the spatial domain for all mobile secondary users while also accurately positioning the stationary secondary user. This is exhibited in the spatial domain by the SU position estimates shown in Figure 30. However, if the decision maker loses track of the channel occupancy of one of the mobile secondary users, the accuracy of the spatial track diminishes until the mobile user is acquired in the frequency domain again. This can be seen in the large spike in distance error of Secondary User 1 during the fifth ESRB localization attempt and the subsequent decrease in distance error in the sixth ESRB localization attempt. It is important to note the loss of track in the frequency domain may not be caused by a direct failure of the ESRB localization scheme. In some cases, whitespace may not be available for the secondary user to occupy. Such a shortfall occurred for Secondary User 2 during the second localization attempt which caused the decision maker to lose track of the user's channel occupancy. Further work is needed to expand the ability of the ESRB localization scheme to perform robust tracking in the spatial domain. Mobility models could be incorporated at the decision maker to make predictions in secondary user behavior [13].

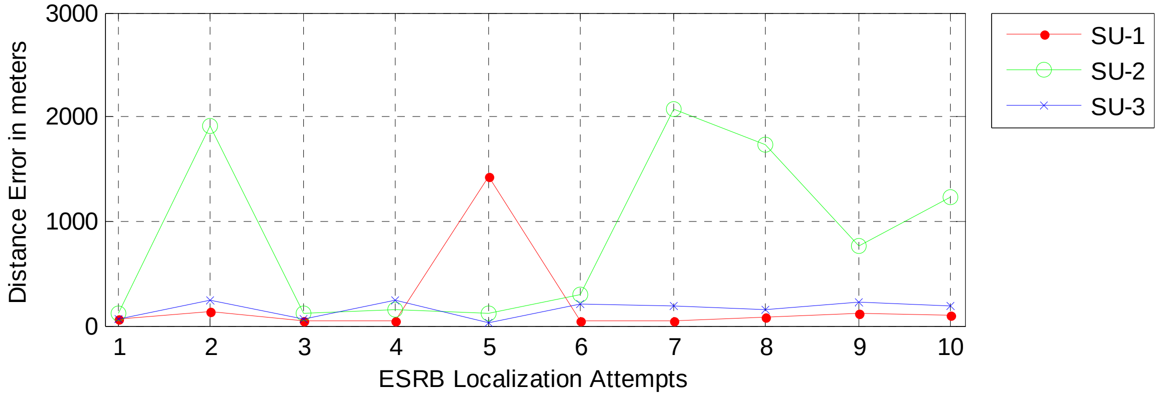

(a)

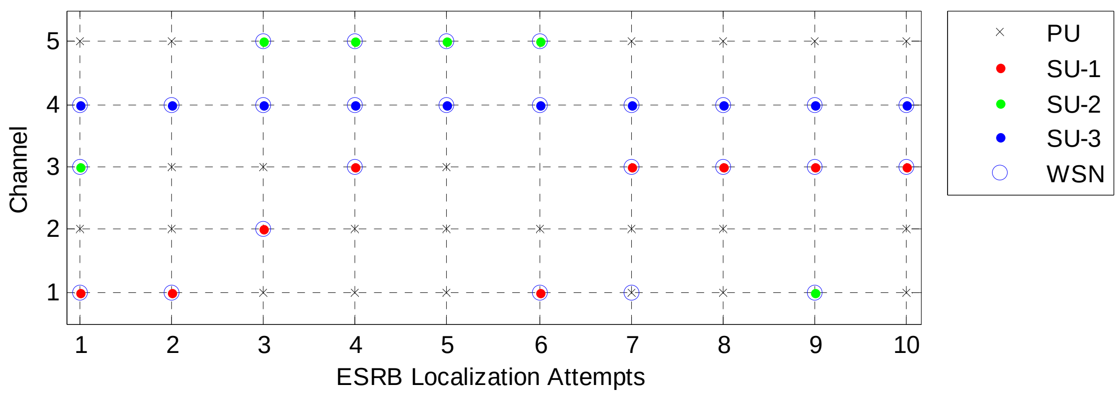

(b)

Figure 31. Multiple mobile and stationary secondary user localization: (a) distance error versus the number of ESRB localization attempts to determine the location of multiple mobile and stationary cognitive radios, (b) channel occupancy versus the number of localization attempts to determine the frequency bands of multiple mobile and stationary cognitive radios.

An overview of the simulation scenario and simulation model used to determine the performance of the ESRB localization scheme under a variety of conditions were provided in this chapter. Specifically, power estimation and the effects of *n*-bit spectrum sensing, the number of spectral scans per superframe, the number of superframes, and the number and position of sensor nodes were examined. The results were the averaged outcomes of a large number of simulation executions. Instantaneous results were also

presented to discuss the effects of frequency and spatial mobility of the secondary user and to demonstrate scalability of the proposed scheme through position estimation of multiple secondary users.

V. CONCLUSIONS

The focus of this thesis was on source localization in a cognitive radio environment. Specifically, how to estimate the position of a cognitive radio using the collaborative spectrum sensing results of a wireless RF sensor network. Three important subtasks identified as crucial components to completing this task were: 1) tracking the frequency bands occupied by the cognitive radio over time, 2) discriminating between primary and secondary users in the environment, and 3) converging onto the true position of the cognitive radio given additional decision data from the sensor network.

An extension of the semi range-based localization algorithm for cognitive radio networks [5], [17] was proposed to accomplish these objectives. Specifically, the practical semi-range based localization algorithm [17], originally proposed for primary user source localization in cognitive radio networks, was extended for cognitive radio source localization. In addition, *n*-bit spectrum sensing, originally proposed for two-bit [22] and three-bit [18] hard combination, was incorporated to improve performance of the proposed ESRB localization scheme. A simulation scenario was introduced to implement the proposed scheme and determine its efficacy under a variety of conditions. The simulation scenario was implemented in the MATLAB programming language through a specific simulation model. Power estimation and the effects of *n*-bit spectrum sensing, the number of spectral scans per superframe, the number of superframes, and the number and position of sensor nodes were examined to determine the effect on the secondary user position estimate. Frequency and spatial mobility of the secondary user were also examined to account for all possible variations in the secondary user's activity. Scalability of the ESRB localization scheme was also addressed with multiple secondary users present in the environment.

A. SIGNIFICANT RESULTS

Over time the proposed ESRB scheme is capable of estimating the frequency band of operation and the location of a cognitive radio. The number of sensor nodes did not directly influence position estimation accuracy; however, adequate separation among

the sensor nodes proved to be a significant factor in the performance of the localization process. Similar to position estimation, power estimation also improved as the number of samples from the sensor network increased. As the number of superframes increased and more decision data became available, the proposed scheme was capable of refining the position estimate using relevant decision data to deliver accurate results.

Alternatively, the use of *n*-bit spectrum sensing significantly improved the performance of the ESRB localization scheme in terms of divergence percentage. The decrease in divergence percentage also directly influenced the overall position estimation error, which allowed the proposed scheme to perform well with a limited amount of decision data from the sensor network.

Finally, through instantaneous results, it was shown the ESRB localization is scalable to localize multiple secondary users in the environment and is capable of accounting for both frequency and spatial mobility when the secondary user is mobile. Limited frequency and spatial tracking was demonstrated for a mobile secondary user on a fixed trajectory at constant speed. Frequency and spatial estimation was accomplished through repeated application of the proposed ESRB localization scheme.

B. FUTURE WORK

Several areas of expansion for future work are offered in this thesis. The incorporation of *n*-bit spectrum sensing into the proposed ESRB localization scheme was used to improve the performance of the iterative NLSM. By weighting the decision data from the wireless sensor network, an accurate initial estimate of the secondary user's position and transmit power can be obtained. The use of *n*-bit hard combination can be examined further to accelerate the spectrum sensing process by reducing the volume of decision data required to form an initial estimate of the secondary user's position and transmit power. Alternative numerical optimization techniques other than the iterative NLSM could also be considered for more effective results.

The simulation scenario and simulation model implemented in this thesis restricted the geography of the primary and secondary user networks to within several thousand meters of each other. However, the range of cognitive radio networks may span

tens or hundreds of kilometers in the real world [19], [29], [31]. Given such potential, the simulation scenario and simulation model can be expanded such that the primary and secondary user's spatial characteristics model real world three-dimensional geography of cognitive radio networks over legacy communication networks. In such a case, the spectrum sensing process represented in the MATLAB programming language can be replaced with real decision data collected from a real world environment.

Limited frequency and spatial tracking was demonstrated in this thesis with a mobile secondary moving along a fixed trajectory at constant speed. However, user activity seldom demonstrates such deterministic behavior in the real world [3]. Therefore, advanced secondary user mobility characteristics can also be implemented in the simulation model to account for random movement at various speeds over time.

The proposed ESRB localization scheme is based on semi range-based localization which is fundamentally a positioning scheme used to localize an emitter of interest at a single point in time [5], [17]. This is a significant limitation when considering a mobile device whose position will change rapidly over time. Ultimately, tracking a cognitive radio is the primary objective of expanding this thesis research. Such a shift would drive examination of alternative localization techniques which are designed to track position over time using a wireless RF sensor network, such as Kalman filtering [13].

THIS PAGE INTENTIONALLY LEFT BLANK

APPENDIX

The selected MATLAB code used to determine the efficacy of the proposed ESRB localization scheme is given in the appendix.

MATLAB CODE TO IMPLEMENT THE EXTENDED SEMI RANGE-BASED LOCALIZATION SCHEME

```
%% Baseline Simulation Model for ESRB Localization Scheme
%  Author: Capt Adams, Agur
%  Purpose: NPS MSEE/EE Thesis
clear all; clc; close all;  % Initialization

%% Variable Workspace
    % Simulation Control
    Simulation = struct('NUMBER', {1}, ...
                        'DURATION', {9000}, ...
                        'time', {1});
    % Primary Users, PU
    PU = struct('QUANTITY', {5}, ...
                'TX_PWR', {18}, ...
                'BUSY_PROB', {0.3}, ...
                'IDLE_PROB', {0.3}, ...
                'MAX_RADIUS', {134e3}, ...
                'MIN_RADIUS', {134e3}, ...
                'MAX_ANGLE', {2 * pi}, ...
                'MIN_ANGLE', {0}, ...
                'history', {0});
    % Secondary Users, SU
    SU = struct('QUANTITY', {3}, ...
                'TX_PWR', {16}, ...
                'CELL_RADIUS', {17e3}, ...
                'MAX_ANGLE', {2 * pi}, ...
                'MIN_ANGLE', {0}, ...
                'history', {0});
    % Wireless Sensor Network, WSN
    WSN = struct('QUANTITY', {50}, ...
                 'MAX_RADIUS', {900}, ...
                 'MIN_RADIUS', {50}, ...
                 'MAX_ANGLE', {2 * pi}, ...
                 'MIN_ANGLE', {0}, ...
                 'PROB_FALSE_ALARM', {0.01}, ...
                 'nBit', {2}, ...
                 'energyThreshold', {0});
    % Decision Maker, DM
    DM = struct('targetAcquired', {0}, ...
                'errorDesired', {1}, ...
                'errorActual', {inf}, ...
                'suHistory', {[]}, ...
                'suFound', {[]}, ...
                'suFinal', {[]}, ...
```

```
                'puPositionError', {1000}, ...
                'suPositionError', {750}, ...
                'divergenceError', {900}, ...
                'aliveError', {1}, ...
                'superframe', {0}, ...
                'SU_TX_AVG_PWR', {17});
    scanningHistory = [];
    % IEEE 802.22 Parameters
    IEEE_802_22 = struct('CHANNEL_NUMBER', {5}, ...
                         'FAST_SENSE_TIME', {1}, ...
                         'FAST_SENSE_PROB', {0.650}, ...
                         'FINE_SENSE_TIME', {25}, ...
                         'FINE_SENSE_PROB', {0.450}, ...
                         'MAC_FRAME_TIME', {100}, ...
                         'SUPERFRAME_TIME', {600});
    % Channel Characteristics and Communications Profile
    Channel = struct('PATH_LOSS_COEF', {0.01}, ...
                     'PATH_LOSS_EXPONENT', {3}, ...
                     'NOISE_VARIANCE', {1e-12}, ...
                     'TIME_BANDWIDTH_PRODUCT', {5}, ...
                     'SHADOW_STD_DEV', {1}, ...
                     'SHADOW_MEAN', {0}, ...
                     'shadow', {0});

%% Simulation Setup
% Place the PU, SU, and sensor nodes in the environment
    % Generate positions for all WSN
    wsnPositions = placeallwsn(WSN);
    % Generate positions for all SU
    suPositions = placeallsu(SU, WSN);
    % Generate positions for all PU
    puPositions = placeallpu(PU, suPositions);
    % Plot the simulation environment
    plotenvironment(wsnPositions, suPositions, puPositions, WSN);
    % Determine the distances from all WSN to all PUs and SUs
    [distanceWSNtoPU, distanceWSNtoSU] =
determinedistanceWSNtoPUandSU(wsnPositions, suPositions, puPositions);

% Allow the PU and SU to occupy the environment
    % Randomly generate the PU spectral occupancy
    [superframeOccupancy, PU.history] = puoccupy(Simulation,
IEEE_802_22, PU);
    % Randomly generate the SU spectral occupancy
    [superframeOccupancy, SU.history] = suoccupy(SU,
superframeOccupancy);
    % Determine energy detection thresholds for all WSN
    WSN.energyThreshold = determineenergythresholds(WSN, Channel);

%% Simulation Execution
while (Simulation.time < Simulation.DURATION)
    % Expand the spectral occupancy to match the number of superframes
    % required to reach the desired sensing periods
    sensingOccupancy = expandoccupancy(IEEE_802_22, DM, PU, SU,
superframeOccupancy);
    % Determine medium scale fading (varies over each localization
```

```
    % iteration)
    Channel.shadow = Channel.SHADOW_MEAN + ...
                     Channel.SHADOW_STD_DEV*randn(1);
    % Perform Spectral Scanning
    [Simulation.time, superframeScanResults] = spectralscanning( ...
                                                       Simulation, ...
                                                              WSN, ...
                                                      IEEE_802_22, ...
                                                          Channel, ...
                                                               DM, ...
                                                               PU, ...
                                                               SU, ...
                                              superframeOccupancy, ...
                                                 sensingOccupancy, ...
                                                  distanceWSNtoPU, ...
                                                  distanceWSNtoSU);
    % Build environment map at DM based on all the WSN results
    [DM.suFound, DM.superframe] = buildenvironmentmap(DM, ...
                                 superframeScanResults, ...
                                                  WSN, ...
                                              Channel, ...
                                          IEEE_802_22, ...
                                         wsnPositions, ...
                                          puPositions);
    % Isolate the spectral scanning results which pertained the SU
    % discovered
    [DM.suHistory, DM.suFound, scanningHistory] =
                                    isolatespectralscanning( ...
                                            scanningHistory, ...
                                      superframeScanResults, ...
                                                        DM);
    % Refine the position estimate based on the aggregated scanning
    % results
    DM.suHistory = positionrefinement(scanningHistory, DM, WSN, ...
                        wsnPositions, Channel, IEEE_802_22);
end
    % Make final decision on number and position of SU
    DM.suFinal = finaldecision(DM, puPositions);

%% Single Simulation Results
    % (Single Simulation Testing) Output final decision on number and
    % position of SU
    outputfinaldecision(DM);
    % (Single Simulation Testing) Calculate distance error
    [suPosError, suPwrError] = calculateerror(suPositions, DM, SU);
    % (Single Simulation Testing) Plot simulation results
    plotresults(PU, SU, DM, suPosError, IEEE_802_22);

%% Multiple Simulation Runs
    % Proceed with additional simulation runs
    finalSimError = [suPosError(DM.superframe), ...
                     suPwrError(DM.superframe)];
    set(0, 'RecursionLimit', Simulation.NUMBER * 50);
    save('ESRB_2A_4SupFrm_10WSN.txt', 'finalSimError', '-append', ...
         '-ascii', '-double', '-tabs');
```

```
load('iTrial');
if (iTrial < (Simulation.NUMBER-1))
    iTrial = iTrial + 1;
    save('iTrial', 'iTrial');
    Base_Model_ESRB
else
    display('Done With Simulation Runs...');
    iTrial = 0;
    save('iTrial', 'iTrial');
    display('Simulation RESET complete...');
end
```

LIST OF REFERENCES

[1] D. Cavalcanti and M. Ghosh, "Cognitive Radio Networks: Enabling New Wireless Broadband Opportunities," Proc. 3rd International Conference on Cognitive Radio Oriented Wireless Networks and Communications, pp. 1–6, 2008.

[2] T. Yucek and H. Arslan, "A survey of spectrum sensing algorithms for cognitive radio applications," IEEE Communications Surveys & Tutorials, vol. 11, no. 1, pp. 116-130, First Quarter 2009.

[3] J. Figueiras and S. Frattasi, Mobile Positioning and Tracking: From Conventional to Cooperative Techniques. John Wiley and Sons, 2010.

[4] J. Mitola and G. Q. Maguire, "Cognitive radio: making software radios more personal," IEEE Personal Communications, vol. 6, no. 4, pp. 13–18, Aug. 1999.

[5] Zhiyao Ma, Wei Chen, K. B. Letaief, and Zhigang Cao, "A Semi Range-Based Iterative Localization Algorithm for Cognitive Radio Networks," IEEE Transactions on Vehicular Technology, vol. 59, no. 2, pp. 704–717, February 2010.

[6] S. Kim, H. Jeon, and J. Ma, "Robust Localization with Unknown Transmission Power for Cognitive Radio," Proc. IEEE Military Communications Conference, pp. 1–6, 2007.

[7] S. Haykin, "Cognitive radio: brain-empowered wireless communications," IEEE Journal on Selected Areas in Communications, vol. 23, no. 2, pp. 201–220, February 2005.

[8] K. Ben Letaief and Wei Zhang, "Cooperative Communications for Cognitive Radio Networks," Proceedings of the IEEE, vol. 97, no. 5, pp. 878–893, May 2009.

[9] R. D. Hinman, "Application of Cognitive Radio Technology to Legacy Military Waveforms in a JTRS (Joint Tactical Radio System) Radio," Proc. IEEE Military Communications Conference, pp. 1–5, 2006.

[10] F. W. Seelig, "A Description of the August 2006 XG Demonstrations at Fort A.P. Hill," Proc. 2nd IEEE International Symposium on New Frontiers in Dynamic Spectrum Access Networks, pp. 1–12, 2007.

[11] P. F. Marshall, "Extending the Reach of Cognitive Radio," Proceedings of the IEEE, vol. 97, no. 4, pp. 612–625, Apr. 2009.

[12] J. B. Bernthal, T. X. Brown, D. N. Hatfield, D. C. Sicker, P. A. Tenhula, and P. J. Weiser, “Trends and Precedents Favoring a Regulatory Embrace of Smart Radio Technologies,” Proc. 2nd IEEE International Symposium on New Frontiers in Dynamic Spectrum Access Networks, pp. 633–648, 2007.

[13] A. Ribeiro, I. Schizas, S. Roumeliotis, and G. Giannakis, “Kalman Filtering in Wireless Sensor Networks,” IEEE Control Systems, vol. 30, no. 2, pp. 66–86, April 2010.

[14] J. Nemeroff, L. Garcia, D. Hampel, and S. DiPierro, “Application of sensor network communications,” Proc. IEEE Military Communications Conference, vol. 1, pp. 336–341, 2001.

[15] Sang Hyuk Lee, Soobin Lee, Heecheol Song, and Hwang Soo Lee, “Wireless sensor network design for tactical military applications: Remote large-scale environments,” Proc. IEEE Military Communications Conference, pp. 1–7, 2009.

[16] Yun Wang, Xiaodong Wang, Demin Wang, and D. P. Agrawal, “Range-Free Localization Using Expected Hop Progress in Wireless Sensor Networks,” IEEE Transactions on Parallel and Distributed Systems, vol. 20, no. 10, pp. 1540–1552, October 2009.

[17] Z. Wang, Z. Feng, J. Song, Y. Hu, and P. Zhang, “A Practical Semi Range-Based Localization Algorithm for Cognitive Radio,” Proc. Vehicular Technology Conference, pp. 1–5, 2010.

[18] V. Sönmezer, M. Tummala, J. McEachen, and A. Adams, “Cooperative wideband spectrum sensing using radio frequency sensor networks,” Proc. 2010 Conference Record of the Forty Fourth Asilomar Conference on Signals, Systems and Computers, pp. 951–955, 2010.

[19] C. Cordeiro, K. Challapali, D. Birru, S. Shankar, and others, “IEEE 802.22: an introduction to the first wireless standard based on cognitive radios,” Journal of communications, vol. 1, no. 1, pp. 38–47, 2006.

[20] K. G. Shin, Hyoil Kim, A. W. Min, and A. Kumar, “Cognitive radios for dynamic spectrum access: from concept to reality,” IEEE Wireless Communications, vol. 17, no. 6, pp. 64–74, December 2010.

[21] H. Celebi and H. Arslan, “Cognitive Positioning Systems,” IEEE Transactions on Wireless Communications, vol. 6, no. 12, pp. 4475–4483, December 2007.

[22] Jun Ma, Guodong Zhao, and Ye Li, “Soft Combination and Detection for Cooperative Spectrum Sensing in Cognitive Radio Networks,” IEEE Transactions on Wireless Communications, vol. 7, no. 11, pp. 4502–4507, November 2008.

[23] Wei Zhang, R. K. Mallik, and K. Ben Letaief, “Cooperative Spectrum Sensing Optimization in Cognitive Radio Networks,” Proc. IEEE International Conference on Communications, pp. 3411–3415, 2008.

[24] A. Ghasemi and E. S. Sousa, “Spectrum sensing in cognitive radio networks: requirements, challenges and design trade-offs,” IEEE Communications Magazine, vol. 46, no. 4, pp. 32–39, April 2008.

[25] I. Guvenc and Chia-Chin Chong, “A Survey on TOA Based Wireless Localization and NLOS Mitigation Techniques,” IEEE Communications Surveys & Tutorials, vol. 11, no. 3, pp. 107–124, Quarter 2009.

[26] N. Patwari, J. N. Ash, S. Kyperountas, A. O. Hero, R. L. Moses, and N. S. Correal, “Locating the nodes: cooperative localization in wireless sensor networks,” IEEE Signal Processing Magazine, vol. 22, no. 4, pp. 54–69, July 2005.

[27] Chao Wang, Kai Liu, and Nan Xiao, “A Range Free Localization Algorithm Based on Restricted-Area for Wireless Sensor Networks,” Proc. 3rd International Multi-Conference on Computing in the Global Information Technology, pp. 97–101, 2008.

[28] G. Chouinard, “802.22 Presentation to the ECSG on White Space,” March 10, 2009.

[29] C. Stevenson, G. Chouinard, Zhongding Lei, Wendong Hu, S. Shellhammer, and W. Caldwell, “IEEE 802.22: The first cognitive radio wireless regional area network standard,” IEEE Communications Magazine, vol. 47, no. 1, pp. 130-138, January 2009.

[30] D. Gurney, G. Buchwald, L. Ecklund, S. L. Kuffner, and J. Grosspietsch, “Geo-Location Database Techniques for Incumbent Protection in the TV White Space,” Proc. 3rd IEEE Symposium on New Frontiers in Dynamic Spectrum Access Networks, pp. 1–9, 2008.

[31] C. Stevenson, C. Cordeiro, E. Sofer, and G. Chouinard, “Functional Requirements for the 802.22 WRAN Standard.doc.” IEEE 802.22 Working Group, November 29, 2006.

[32] Youping Zhao, L. Morales, J. Gaeddert, K. K. Bae, Jung-Sun Um, and J. H. Reed, “Applying Radio Environment Maps to Cognitive Wireless Regional Area Networks,” Proc. 2nd IEEE International Symposium on New Frontiers in Dynamic Spectrum Access Networks, pp. 115–118, 2007.

[33] C. T. Kelley, Iterative methods for optimization. SIAM, 1999.

THIS PAGE INTENTIONALLY LEFT BLANK

INITIAL DISTRIBUTION LIST

1. Defense Technical Information Center
   Ft. Belvoir, Virginia

2. Dudley Knox Library
   Naval Postgraduate School
   Monterey, California

3. Marine Corps Representative
   Naval Postgraduate School
   Monterey, California

4. Director, Training and Education, MCCDC, Code C46
   Quantico, Virginia

5. Director, Marine Corps Research Center, MCCDC, Code C40RC
   Quantico, Virginia

6. Marine Corps Tactical Systems Supper Activity (Attn: Operations Officer)
   Camp Pendleton, California

7. Prof. Clark Robertson
   Department of Electrical and Computer Engineering
   Naval Postgraduate School
   Monterey, California

8. Prof. Murali Tummala
   Department of Electrical and Computer Engineering
   Naval Postgraduate School
   Monterey, California

9. Prof. John McEachen
   Center for Cyber Warfare
   Naval Postgraduate School
   Monterey, California

10. Prof. Frank Kragh
    Department of Electrical and Computer Engineering
    Naval Postgraduate School
    Monterey, California

11. Prof. Peter Ateshian
Department of Electrical and Computer Engineering
Naval Postgraduate School
Monterey, California

12. Donna Miller
Department of Electrical and Computer Engineering
Naval Postgraduate School
Monterey, California

13. Capt. Agur Adams
Department of Electrical and Computer Engineering
United States Naval Academy
Annapolis, Maryland